FINAL REPORT

METEOROID IMPACT FLASH ANALYZER

R134/FR2

SUBMITTED TO

NATIONAL AERONAUTICS AND SPACE ADMINISTRATION,
MANNED SPACECRAFT CENTER,
HOUSTON, TEXAS

CONTRACT NO. NAS9-8788

PREPARED BY

B. JEAN
R. ALEXANDER

17 MAY 1971

Computing Devices of Canada Limited
a subsidiary of
CONTROL DATA CORPORATION

TABLE OF CONTENTS

TABLE OF CONTENTS (Continued)

TABLE OF CONTENTS (Continued)

ABSTRACT

This report is submitted to NASA MSC Houston in compliance with the requirements of a research program aimed at the determination of a correlation between the impact flash radiative properties and the impacting projectile characteristics. The research described herein is a complement to a previous more comprehensive study which was reported in December 1969. The goal of the present extension phase is to clarify the nature of the radiation emitted in three narrow band spectral windows and to build up statistics about the projectile parameters influence on flash characteristics.

1. INTRODUCTION:

In 1969 a research program was conducted in our laboratory for the NASA MSC in Houston. Its primary objective was to define empirical relationships for the dependence of time resolved intensity of the radiation emitted in hypervelocity impact on the projectile size and velocity when a meteorite material projectile impacts on a cadmium target. A secondary research task was to study the feasibility of identifying the type of meteorite material from a measurement of its impact flash signature at certain spectral wave length windows. The results of this research program have been reported in Reference 1.

It was concluded at the end of the above program that the determination of the projectile parameters (size, velocity, material) from the flash signature is feasible. However, the empirical relationships relating flash intensity and rate of change of intensity to the projectile velocity and size were subject to uncertainty due to the large spread of the data collected. It was then decided to collect more data in the case of the Canyon Diablo meteorite projectile to clarify the influence of the velocity and size of the projectile on the impact flash characteristics. This data collection has been the subject of a phase of the present program. The influence of the target orientation on the impact flash has also been evaluated.

Meteorite type identification by impact flash intensity analysis did not prove successful in the previous program because of the experimental observation of indiscriminate radiation in every spectral window irrespective of the material used in the projectile. This observation re-opened the question of the nature and origin of the impact flash and indicated the need for clarification of the type of radiation emitted (continuous or line emission). Three phases of the present program have been devoted to this end. The first phase resolves the spectral emission inside three selected spectral windows. The second phase

assesses the time integration of the line emission as a means of material identification. A third research task evaluates the importance of ionization in the impacts of MgLi projectiles launched at higher velocities.

During the firing program a breadboard logic circuit with digital flash intensity output was developed. This should satisfy the requirements of interface between radiation monitors and space telemetry systems.

2. PARAMETRIC STUDIES

The purpose of the parametric study task was to gather new data points in order to achieve a better statistical correlation between the flash properties and the projectile parameters. The intensity I and rate of change of intensity $\frac{dI}{dt}$ of the impact flash at four spectral windows were monitored by a spectral analyzer built in the course of the previous program and which has been described in reference 1. The results were studied as a function of the projectile velocity V diameter d and target inclination θ such that an empirical relationship could be established relating I, and $\frac{dI}{dt}$ to V, d and θ. The projectiles were spheres turned from a Canyon Diablo meteoritic sample. They were launched by a ½" light gas gun against a polished cadmium target mounted in a firing range whose ambient pressure was maintained under vacuum to better than 5×10^{-5} millimeters of Hg. The flash analyser monitored three narrow spectral bands 85Å wide containing emission lines from the cadmium target material at 5085Å, 3610Å, and 3261Å. A fourth spectral band, was monitored which does not contain cadmium emission. This band was centered at 4900Å.

The results of the experimental program are listed in Tables 1, 2, and 3. The following three parameters have been studied; velocity, size and angle of impact.

2.1 Velocity Dependence

The influence of the velocity on impact flash characteristics has been studied for a 1.2 millimeter diameter projectile. Five new data points have now been added to the six data points which were collected in the previous program and which were reported in Reference 1. For each wavelength, a graph of log intensity and log rate of change of intensity vs log projectile velocity was drawn. A best visual fit slope to the total number of points accumulated over the two experimental programs involving Canyon Diablo projectiles has been drawn. There is good indication that the empirical laws describing the relationship between I, $\frac{dI}{dt}$ and velocity can be expressed, at various wavelengths, according to the following table.

λ (A°)		
3261	$I \propto V^{9.1(+.2,-.4)}$	$dI/dt \propto V^{8.2(+0,-1.1)}$
3610	$I \propto V^{10.2(+.3,-.4)}$	$dI/dt \propto V^{8.2(+.6,-0)}$
4900	$I \propto V^{7.9(+.4,-5)}$	$dI/dt \propto V^{8.2(+.9,-.5)}$
5085	$I \propto V^{9.1(+0,-.6)}$	$dI/dt \propto V^{8.2(+.6,-1.7)}$
Average	$I \propto V^{9.1}$	$dI/dt \propto V^{8.2}$

The exponent has been chosen from a set of many possible slopes estimated by 3 different interpreters. The results are presented in Figures (1 to 8). These results may appear at variance with the previous work reported in References 1 and 2. However, the value of the exponent then measured, as it was explained at the time thesreport was written, showed fluctuations which were within the limits of the values chosen in the present report. The variation of exponent with wavelength which was previously reported is confirmed here for the case of I vs V. However the exponents in the empirical relations between $\frac{dI}{dt}$ and V were so similar that the mean value (8.2) was chosen for all wavelengths.

2.2 Diameter Dependence

The dependence of the flash intensity monitored in the four spectral windows on projectile diameter has also been verified using again a Canyon Diablo meteorite projectile launched against a cadmium target at 5.5 km/sec. Because of the limited repeatability of the exact velocity the results given in Figures (9 to 16) and Table 2 expressing the dependence of I and dI/dt with diameter have been normalized to a velocity of 5.5 km/sec using the velocity dependence laws defined on the previous page.

Here again the new data points have been added to the data collected in the previous program. A best visual fit straight line was faired through the plots of log I and log dI/dt vs log diameter to arrive at the diameter exponents in the empirical relations relating I and dI/dt to the projectile diameter. A large scatter in intensity readings at each diameter is still apparent as it was in the previous report. Because of this scatter it was difficult to justify individual slopes for each wavelength and therefore the average values of numerous independent straight line plots was chosen.

The diameter exponent was $3.4 \pm \begin{smallmatrix} .3 \\ .4 \end{smallmatrix}$ in the relation for I vs d and $3.1 \pm \begin{smallmatrix} .3 \\ .2 \end{smallmatrix}$ in the dI/dt vs d relation for all four monitored wavelengths: 3261Å, 3610Å, 4900Å and 5085Å.

$$I \propto d^{3.4\ (+.3,\ -.4)}, \qquad dI/dt \propto d^{3.1(+.3,\ -.2)}$$

2.3 Angle of Incidence Effect

The effect of the target orientation relative to the projectile line of flight on the flash characteristics has been experimentally evaluated. For this the cadmium target was rotated around an axis passing through the impact flash analyzer. The projectile consisted of a sphere of Canyon Diablo meteorite material. It was launched at 5.5 km/sec against the cadmium target. The results of the experiments are tabulated in Table 3. The plots of the variation of intensity and rate of change of intensity with target inclination from the normal to the line of flight are represented in Figures 17 and 18 for the four wavelength bands monitored. These figures indicate that both the flash intensity and the rate of change of intensity decrease at least one order of magnitude as the impact angle of incidence varies from 0 to 30 degrees.

To test the hypothesis that I and dI/dt are functions of the component of velocity normal to the target, they were normalized by the factor $[\frac{5.5}{V \cos \theta}]^{\beta}$ where β is the appropriate velocity exponent derived previously for each wavelength. The average values of the normalized I and dI/dt for all four wavelengths were then plotted relative to their arbitrary values at θ equal to 0 degrees (see Figures 19 and 20). It became obvious that the normalized values of I and dI/dt remained constant over the range of target inclination from 0 to 20 degrees. This indicated that the flash mechanism is related to the component of the velocity normal to the target plane.

3. PHENOMENOLOGICAL STUDIES

3.1 Copper-Cadmium Impact

In order to demonstrate the feasibility of meteoritic material indentification by detection of emission from elements which would uniquely determine their presence in the impact flash, it was suggested that spectral windows containing line emissions of these elements be monitored. The concept was tested in the previous program.

One of the tests of that program in launching a Cu sphere against a cadmium target and monitoring the radiation at the spectral windows corresponding to emission of elements present in meteoritic material only; not in copper. Since radiation in these narrow bands had not been spectrographically observed in these types of firings involving copper, no responses were to be expected from the analyzer monitoring the chosen 100Å wide bands. However radiation was effectively detected by the analyzers. This observation reopened the question of the understanding of the impact flash spectral characteristics.

In order to reach a conclusion about the spectral properties of the impact flash an experimental program was designed by which three of the 100Å wide spectral bands were to be scanned by a 20Å wide window. A Czerney-Turner direct reading polychromator was used in the course of the experiment. The three spectral windows covered were centered at 2478Å, 2707Å and 2866Å. While constant projectile launch conditions were maintained for a number of firings,

the spectrum was displaced each time by 20Å in order to monitor the different steps in the 100Å wide bands. See Figure 21. As seen in Figure 21 a discontinuous spectral distribution has been detected in the three selected wavelength bands.

It appears that inside the three 100Å wide spectral bands the presence of radiation due to ionized copper and cadmium as well as possible impurities like magnesium and silicon has been detected. These emissions are too weak to be detected photographically but are detectable by a sensitive photomultiplier. According to results of this experiment very little seems to be contributed by the continuum radiation often observed at the impact point as compared to line emission since no radiation was detected for certain positions of the exit slit. It can be concluded from this experiment that the sensitivity of the photo detector may easily falsify the interpretation of the identification since impurities as well as low probability transitions are detected by the monitor.

The time integrated radiation which has been readily detected by spectrographic techniques could be used for uniquely determining the presence or absence of a given element in the projectile or the target. This technique is applicable in the laboratory where the projectile can be large enough to produce a detectable amount of radiation and where the impact location can be fairly well controlled in order to gain and collect as much radiation as possible. It has been demonstrated that it is not feasible to transfer spectrographic techniques to a space environment where the projectile although travelling faster, is much smaller and where the impact point is beyond our control. To avoid this difficulty it was suggested that the line identification monitoring photomultiplier give a time integrated response to the radiation emitted in the impact flash at a specific wavelength. The output of a photomultiplier was modified in order to give such a response. Since this new intensity integrator package was ready for the Canyon Diablo - Cadmium impact experiment the photodetector served to monitor the wavelength band which was defined to identify the presence of iron at 3735Å. The results are given in Figure 22.

3.1.1 Time Integrated Radiation Monitor

The voltage output from a photomultiplier monitoring emission at

3735Å was integrated over the 50 μ seconds immediately after spike formation at impact of Canyon Diablo material on cadmium. Satisfactory results were obtained from five shots. See Figure 22 and Table 1. The output voltage from the integrator at 50 μ seconds was normalized to a common aperture diameter of 100 μ, projectile diamter of 1.2 mm, and target inclination of 0^{o} and then plotted against projectile velocity.

According to the 5 data points available, the integrated flash intensity at 3735Å for Canyon Diablo material impacting cadmium can be expressed as a function of projectile velocity by the following expression:

$$\int_{t=0}^{50\ \mu\ \text{sec}} I\ dt \quad \propto \quad V^{6.1}$$

Monitoring of wavelength bands which do not contain any line emissions could have led to more conclusive results on the relative capability of the integrating circuit. This was difficult to achieve with a Canyon Diablo meteorite projectile characterized by the presence of iron and nickel for which spectra are very complex.

3.2 Influence of Ionization for High Velocity Impact

The presence of a high degree of ionization has been spectroscopically observed at ComDev for the impact of a MgLi projectile impacting a cadmium target at 10 km/sec. In order to verify if this effect would be detrimental to the radiative characteristics as a function of projectile parameters, a short experimental program was undertaken. It consisted of studying the impact flash produced by a MgLi projectile launched by means of an accelerator coupled to a conventional light gas gun. The choise of MgLi was dictated by its low density and its ability to withstand the stresses imposed by high acceleration.

In order to obtain a comprehensive study of MgLi impact flash characteristics, 5.2 mm spheres were impacted at velocities ranging from 4 km/sec to 8 km/sec. Equivalent mass cylindrical MgLi projectiles were successfully launched at velocities of 7.6, 9.1 and 9.5 km/sec. However, the measurements of the flash intensities and rates of change of intensity for cylinders were erratic. Observation of

the open shutter camera integrated flash pictures revealed that the cylinder was impacting at varying angles of attack. Shape effect experiments in the previous phase of the program had demonstrated that the nature of the impact mechanism is strongly dependent on the radius of curvature and the orientation of the projectile surface at the point of impact. By analogy, the flat surface of the cylindrical projectile would produce variations in flash characteristics if it did not impact in exactly the same manner in each experiment.

The flash intensity and rate of change of intensity are plotted in Figures 23 to 30 for only one of the cylindrical projectiles to show the variance from spherical projectile data. It was not possible to distinguish a flash spike for the other two cylinder impacts. Because it was not possible to successfully launch spherical projectiles from the accelerator, reliable data points at velocities above 8 Km/sec are not available.

In the case of MgLi sphere impacts, the five data points which have been collected indicate that the intensity varies as approximately the 7th or 8th power of the velocity depending on the wavelength being monitored. See Figures 23 to 26. The variation of the rate of change of intensity, $\frac{dI}{dt}$, with velocity at four different wavelengths is between the 6.1 and 7.7 power of the velocity. See Figures 27 to 30. These powers were obtained from the average of three independent readings of the slope of log intensity and log rate of change of intensity versus log velocity. Because there were at most, only five data points for each wavelength, it was difficult to settle on a particular slope. In Figures 23 to 26 an average slope of7.5 has been plotted representing a variation of flash intensity as the 7.5 power of projectile velocity for all wavelengths monitored. The average exponent of $\frac{dI}{dt}$ versus V was 6.7, as may be seen in Figures 27 to 30.

The presence of ionized species in the spectrum has been readily observed for the impact of a MgLi sphere at 7.0 km/sec. A spectrum distribution for an impact 7.7 km/sec is shown in Figure 31, in which many ionized cadmium transitions have been detected at 2573Å, 2748Å, 3298Å and 4415Å. Still more ionized Mg transitions are also present. The presence of impurities like Al., Cu., Ca and other unidentified species render complex the flash spectrum which otherwise should be fairly simple. The emission of these species in the monitored spectral windows does not, however, seem to affect the measured spike intensity variation with velocity since with any material one always finds approximately the same type of empirical relationship irrespective of the type of material used.

4.0 BREADBOARD CIRCUITS - FEASIBILITY MODELS

4.1 Introduction

One of the objectives of the program was to develop and demonstrate circuits capable of converting flash signals into electrical signals for transmission by standard NASA telemetry. The circuits developed and tested during the firing program have accepted and converted photo-multiplier output signals to d.c. signals characteristic of specific peak intensity and integrated signal levels.

The conversion to specific d.c. signals has been taken as adequate demonstration that the data can then be converted into any standard form for telemetry, since bandwidth requirements would then be minimal. In addition the data can be stored by any of the standard computer or other memory techniques, and read out into the telemetry as required.

No attempt has been made to develop circuitry for absolute minimum power consumption or for space environment: the breadboards are strictly lab category. Detailed design for a satellite package may employ the techniques demonstrated during the program however, with due regard to factors of circuit response, dynamic range and radiation hardening.

4.2 Peak Detector - Quantizer Circuit

The circuit is designed to detect and quantize the intensity signal peak value, and to display the signal level in a d.c. form. The derived unique d.c. signal can be converted to any digital code form suitable for storage and subsequent transmission by any standard telemetry technique.

The design of the circuit was oriented to the firing program and has been tested during the firings. The circuit presented is the latest and most successful one and fulfills its functions satisfactorily.

The circuit in its final form comprises a divider string designed to be driven by a 50 ohm line, a series of J-K flip-flops, lamp drivers and lamps, sundry gates, and two switches. One switch peforms the "Reset" functions, the other permits sampling of the integrator circuit output signal.

A 28 volt stabilized power supply is required: the voltage should be adjusted to provide a 3.50 volt reading ($\pm$ 0.03V) at the test point.

4.3 Circuit Operation

The circuit operation is as follows: with power on the "Reset" switch is operated to ready the unit for data. A negative pulse signal fed into the "Pulse" terminal will be applied to the flip-flop toggle inputs in progressively smaller proportions down the divider chain. Q0 will trigger from signals greater than 50 millivolts, Q1 from 200 mv, Q2 from 400 mv, Q3 from 800 mv, Q4 from 1.6 volts and Q5 from 3.2 V. (The divider chain has been driven from a 50 ohm signal line and was designed for this source impedance).

A pulse of 2.3 volts peak will therefore trip flip flops from Q0, Q1, Q2, Q3 and Q4. A pulse of 1.2 volts peak will trip Q0, Q1, Q2, Q3.

The triggering of a flip-flop results in an "on" signal going to the corresponding lamp driver, and since the flip-flop remains in the triggered state until reset, the highest order Q light activated indicates the signal level. For data storage purposes the signals could be fed to exclusive OR gates to generate a unique digital code for the Q level indicated.

The circuit may also be driven by the integrator circuit. In this mode the integrator output is tied to C8 through diode CR14, and since the integrator holds its charge for several minutes the peak Q level can be read off, the "Reset" button pushed and released, and the "Read Integral" button

operated. The d.c. level appearing on C8 is then classified by the quantizer circuit and the Q level corresponding to the integrated signal level may be read out. The specific trigger levels remain stable within an 8 millivolts range, provided the power supply is stabilized to conventional laboratory bench supply standards.

4.4 Integrator Circuit

The circuit effectively presents the photo multiplier mode with a capacitive load of 1000 picofarads shunted by several thousand megohms. Since the leakage currents are extremely low the accumulated charge acquired during a flash results in a voltage being held by the storage capacitor for a lengthy period.

The first transistor is an insulated dual gate field effect device of the B type offering extremely high input resistance. It is operated as an augmented emitter follower in conjunction with the 2N2907A.

Zero signal offset from ground may be set by adjusting the bias of gate 2 with the 50K multi turn potentiometer.

A radiometric calibration of the photo multiplier - integrator module may be effected by shorting the "Photometric Calibration" terminal to ground while performing a normal photo multiplier sensitivity calibration. The value of 100K load resistor permits currents of 10 micro-amps to develop 1 volt signals: this was considered sufficiently low to avoid fatigue seriously affecting the calibration.

The integrator module alone may be calibrated either by injecting charges from a charge calibrator into the input, or by imposing known d.c. signals into the input. (One volt signal corresponds to 1000 pico coulombs charge on a 1000 pico farad capacitor.) A plot of the breadboard characteristic

with d.c. inputs is shown in Figure 34.

Tests with a fast rise pulse generator diode coupled to the input and set to give a 500 cycle per second pulse rate resulted in the integrator output developing a clean staircase output wave up to the point of saturation. Pulses of two volts amplitude fed through a 1K series resistor were employed for the test.

The circuit accepts only negative signals, has a gain of 0.978, and responds to signals with rise times less than 30 nano seconds. A 20 volt power supply, isolated from ground, is required. The circuit diagram is shown in Figure 33.

5. CONCLUSIONS

Canyon Diablo meteorite projectiles have been impacted on cadmium targets to further clarify the influence of projectile size, velocity and angle of incidence on the impact flash signature. Empirical formulae relating flash spike intensity and rate of change of intensity to projectile diameter and velocity have been developed from observations of radiation at four spectral windows (3261Å, 3610Å, 4900Å and 5085Å).

$$I \propto V^{\beta}$$

$$\beta 3261 = 9.1$$
$$\beta 3610 = 10.2$$
$$\beta 4900 = 7.9$$
$$\beta 5085 = 9.1$$

$$\frac{dI}{dt} \propto V^{8.2}$$

$$I \propto d^{3.4}$$

$$\frac{dI}{dt} \propto d^{3.1}$$

According to the data collected, the velocity exponent in the intensity relationship varies with the wavelength being monitored. It was not possible to detect a variation in velocity for the dI/dt relationship. The diameter exponent also remains constant for all four wavelengths in each of the intensity and rate of change of intensity relationships.

The angle of incidence of the projectile on the target has a definite effect on the intensity and rate of change of intensity of the impact flash. Both I and dI/dt decrease by about a factor of ten as the angle of incidence is increased from 0 to 30 degrees. This suggests that the angle of incidence should be limited to 20 degrees or less to minimize errors in the determination of projectile diameters.

When copper spheres were launched against cadmium a discontinuous spectral distribution was observed in three 100Å wide spectral windows corresponding to emission of elements present in the meteoritic material. Weak emissions of copper, cadmium and impurities were detected by the sensitive photodetectors whereas photographic processes would not have been capable of picking them up. These results suggest that continuum radiation is much less important than line emission in impact flash. It was therefore decided to integrate, with respect to time, the output from a photomultiplier monitoring a particular

wavelength to determine the presence or absence of a given element in the projectile or target. The technique of the photomultiplier signal integration was tested at the very end of the program. A firm conclusion on the behaviour of the particular circuit could not be reached because only a single material was used as the projectile. The suggested method of identification remains however justified. Spectral line emissions which are pertinent to the elements present in the projectile had been spectrographically observed by time integration of the line radiation on photographic plates. Achievement of the time integration of the same lines by a photomultiplier should lead to the detection of the presence or absence of the element in the collision. This is the concept behind the use of a time integrating technique to achieve identification of the type of meteorite. The circuit remains to be tested for different projectile material impacts.

MgLi spheres were launched at high velocity into cadmium targets to study the influence of ionization in high velocity impacts. Attempts to use an accelerator to increase projectile velocity had to be abandoned when it was found that the necessary cylindrical projectiles produced erratic impact flash characteristics. Available data indicated that the impact flash intensity varies as the 7.5 power of projectile velocity whereas the rate of change of intensity is proportional to the 6.7 power of velocity.

A typical spectral distribution produced at the impact of MgLi on cadmium indicates the presence of ionized species. These species do not however seem to have a large effect on the measured spike intensity since the same types of empirical relationships exist between I, dI/dt and projectile velocity regardless of projectile composition.

Late in the firing program, both the integrator package and the flash peak detector - quantizer circuits were developed. Results of the bench and subsequent firing tests indicate that an effective interface between the radiation monitors and existing space telemetry systems is feasible.

6. NOMENCLATURE

I	Intensity
$\frac{dI}{dt}$	Time Rate of Change of Intensity
V	Velocity
θ	Angle of Inclination of Target
d	Diameter of Projectile
β	Constant Used as Exponent.

7. REFERENCES

1. Jean, B., Henshaw, H. — Meteoroid Impact Flash Analyzer. ComDev Report R134/FR1, NASA Contract No. NAS9-8788, December 1969.

2. Rollins, T.L., Jean, B. — Impact Flash for Micrometeoroid Detection. ComDev Report 9899/FR1, NASA Contract No. NAS9-6790, May 1968.

TABLE I

PROJECTILE VELOCITY INFLUENCE ON FLASH CHARACTERISTICS

1.2 mm DIAMETER CANYON DIABLO ON CADMIUM

SHOT NO.	379	380	382	383	384
PROJECTILE VELOCITY (Km/sec)	5.99	6.90	5.43	4.19	3.44
PROJECTILE MASS (mgr)	6.85	8.18	6.85	7.20	5.80
5085Å I, $\mu w/cm^2$ @ 1 M	89.1	217.	32.3	--	6.9
dI/dt, $\mu w/cm^2$ usec @ 1M	1845.	1425.	565.	--	90.3
3610Å I, $\mu w/cm^2$ @ 1M	171.4	314.	57.5	--	--
dI/dt, uw/cm^2 usec @ 1M	2223.	4988.	972.	--	--
4900Å I, $\mu w/cm^2$ @ 1M	86.2	151.	32.2	25.6	1.4
dI/dt, $\mu w/cm^2$ usec @ 1M	1769.	4430.	817.	573.	--
3261Å I, $\mu w/cm^2$ @ 1M	25.3	--	--	8.6	--
dI/dt, $\mu w/cm^2$ usec @ 1M					
3735Å INTEGRATOR PACKAGE SIGNAL PEAK, VOLTS @ 100 μ aperture	--	--	3.6	.65	.21

TABLE 2

PROJECTILE DIAMETER INFLUENCE ON FLASH CHARACTERISTICS

CANYON DIABLO ON CADMIUM

SHOT NO.		379	385	387
PROJECTILE DIA (mm)		1.2	2.2	4.8
PROJECTILE MASS (mgr)		6.85	46.4	552.8
PROJECTILE VELOCITY (Km/sec)		5.99	5.08	5.12
5085Å	I, $\mu w/cm^2$ @ 1M	89.1	143.	1620.
	dI/dt, $\mu w/cm^2 usec$ @1M	1845.	1315.	18933.
	$I(5.59/V)^{9.1}$	47.2	342.	3596.
	$dI/dt(5.59/V)^{8.2}$	1052.	2880.	38813.
3610Å	I	171.4	22.5	1736.
	dI/dt, $\mu w/cm^2 usec$ @ 1M	2223.	143.	9530.
	$I(5.59/V)^{10.2}$	84.0	59.6	4253.
	$dI/dt(5.59/V)^{8.2}$	1267.	313.	19537.
4900Å	I	86.2	58.2	1510.
	dI/dt, $\mu w/cm^2 usec$ @ 1M	1769.	1752.	12238.
	$I(5.59/V)^{7.9}$	50.0	124.	3020.
	$dI/dt(5.59/V)^{8.2}$	1008.	3837.	25088.
3261Å	I	25.3	15.6	810.
	dI/dt, $\mu w/cm^2 usec$ @ 1M	390.	480.	8868.
	$I(5.59/V)^{9.1}$	13.4	37.0	1798.
	$dI/dt(5.59/V)^{8.2}$	222.	1051.	18179.

TABLE 3

TARGET ORIENTATION INFLUENCE ON FLASH CHARACTERISTICS

CANYON DIABLO ON CADMIUM

SHOT NO.		318	379	390	391	392
TARGET INCLINATION (deg)		0	0	10	20	30
PROJECTILE DIAMETER (mm)		1.2	1.2	1.5	1.5	1.2
PROJECTILE MASS (mgr)		7.35	6.85	15.41	14.12	8.58
PROJECTILE VELOCITY (Km/sec)		7.29	5.99	4.70	5.25	4.97
5085Å	I, $\mu w/cm^2$ @ 1M	440.9	89.1	2.7	35.8	.7
	dI/dt, $\mu w/cm^2$ usec @ 1M	3644.5	1845.	57.9	1050.	19.5
	$I(5.5/V)^{9.1}\ (1.2/d)^{3.4}$	35.3	41.0	5.2	25.8	1.7
	$dI/dt(5.5/V)^{8.2}\ (1.2/d)^{3.1}$	360.8	917.	105.4	770.7	47.0
3610Å	I, $\mu w/cm^2$ @ 1M	504.4	171.4	37.2	44.9	.9
	dI/dt, $\mu w/cm^2$ usec @ 1M	11762.	2223.	897.	680.	65.5
	$I(5.5/V)^{10.2}\ (1.2/d)^{3.4}$	30.3	72.0	86.7	33.7	2.6
	$dI/dt(5.5/V)^{8.2}\ (1.2/d)^{3.1}$	1164.4	1105.	1632.5	499.	157.9
4900Å	I, $\mu w/cm^2$ @ 1M	368.8	86.2	10.6	-	1.1
	dI/dt, $\mu w/cm^2$ usec @ 1M	4489.9	1769.	278.	-	48.
	$I(5.5/V^{7.9}\ (1.2/d)^{3.4}$	40.6	44.0	17.2	-	2.4
	$dI/dt,\ (5.5/V)^{8.2}\ (1.2/d)^{3.1}$	444.5	879.	506.	-	115.7
3261Å	I, $\mu w/cm^2$ @ 1M	394.2	25.3	4.1	3.6	.24
	dI/dt, $\mu w/cm^2$ usec @ 1M	6975.4	390.	103.5	60.6	56.8
	$I(5.5/V)^{9.1}\ (1.2/d)^{3.4}$	31.5	11.6	8.0	2.6	.60
	$dI/dt(5.5/V^{8.2}\ (1.2/d)^{3.1}$	690.6	194.	188.4	44.5	135.9

TABLE 4

SPECTRAL RESOLUTION WITHIN THREE 100Å WIDE SPECTRAL WINDOWS

1.2MM COPPER SPHERES IMPACTING CADMIUM

SHOT NO.	348	349	351	352	356	357	358
Projectile Velocity (Km/sec)	6.13	5.81	5.95	5.87	5.83	5.87	5.93
Projectile Mass (mgr)	6.89	6.99	9.09	7.62	8.92	10.62	7.60
PM 5 λ (Å)	2469.4	2469.4	2449.4	2429.4	2489.4	2509.4	2449.4
V (mV)	-	-	40	40	9	6	6
PM6 λ (Å)	2737.6	2737.6	2717.6	2697.6	2757.6	2777.6	2717.6
V (mV)	-	-	-	40	100	5	5
PM7 λ (Å)	2856.7	2856.7	2836.7	2816.7	2876.7	2896.7	2836.7
V (mV)	35	70	120	80	9	1	5
PM8 λ (Å)	3610	3610	3610	3610	3610	3610	3610
V (mV)	35	55	12	-	12	20	-

TABLE 5

IONIZATION INFLUENCE ON FLASH CHARACTERISTICS IN MGLI IMPACTS

MAGNESIUM LITHIUM ON CADMIUM

SHOT NO.	364	365	367	368	369	370
Projectile Velocity (Km/sec)	5.67	6.76	3.74	7.12	7.66	7.58
Projectile Mass (mgr)	103.3	103.2	104.1	103.2	103.0	100.0
Projectile Shape	Sphere	Sphere	Sphere	Sphere	Sphere	Disc
Projectile Diameter (mm)	5.2	5.2	5.2	5.2	5.2	.230 dia/.103
5085Å I, $\mu w/cm^2$ @ 1M	156.	636.	11.6	263.	3860.	110.
dI/dt, $\mu w/cm^2$ μsec @ 1M	1509.	4666.	107.5	2650.	28529	1602.
3610Å I, $\mu w/cm^2$ @ 1M	319.	903.	18.	698.	2440.	201.
dI/dt, $\mu w/cm^2$ μsec @ 1M	5347.	10035	330.	11510.	32594	1549.
4900Å I, $\mu w/cm^2$ @ 1M	224.5	725.	9.7	417.	2535.	35.
dI/dt, $\mu w/cm^2$ μsec @ 1M	4437.	7261.	157.6	8338.	15736.	787.
3261Å I, $\mu w/cm^2$ @ 1M	125.	259.	11.0	500.	1400.	-
dI/dt, $\mu w/cm^2$ μsec @ 1M	2238.	5005.	241.8	7712.	26784.	-

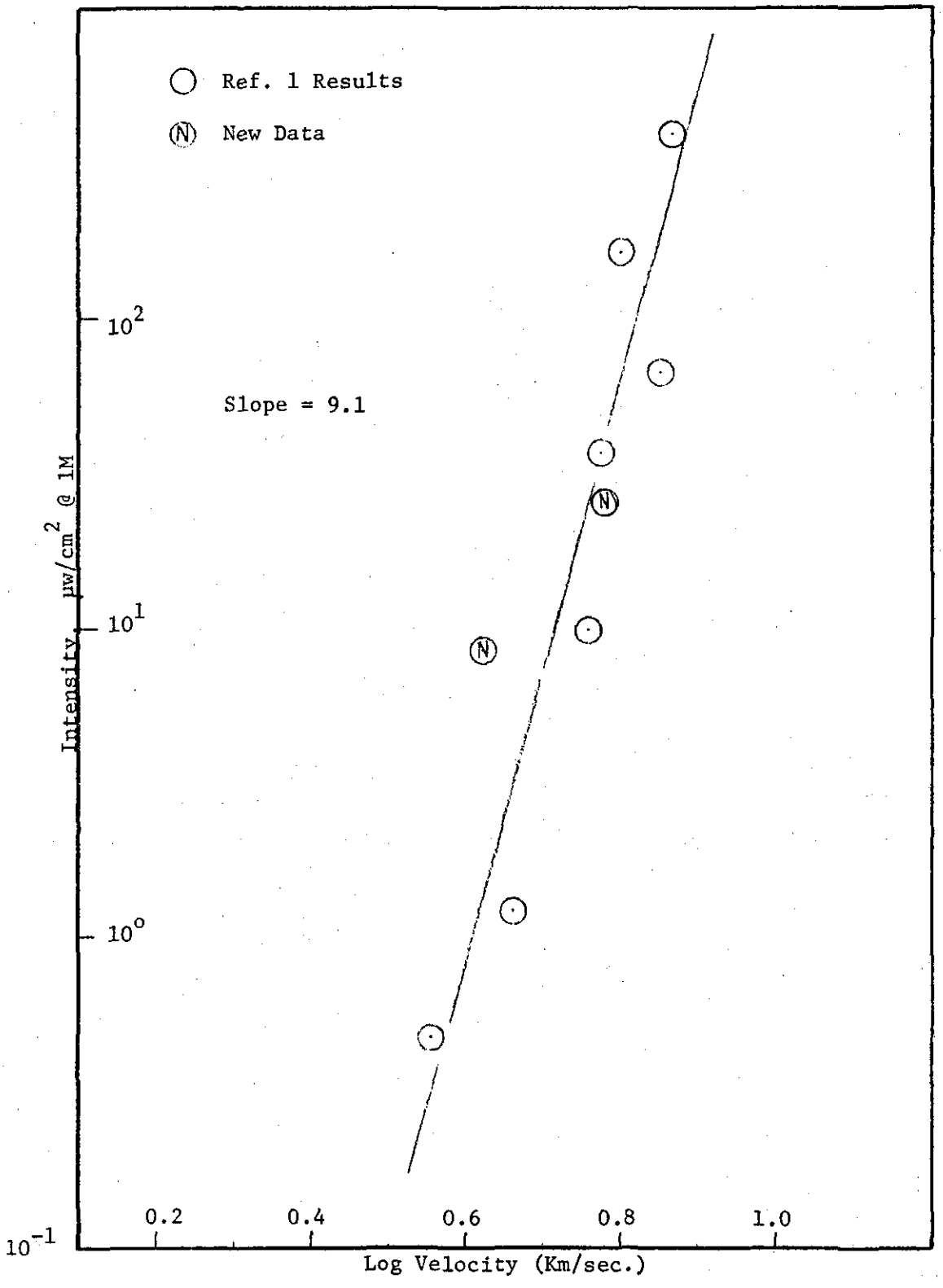

Figure 1. Spike Intensity Variation with Velocity at 3261Å for a 1.2 Millimeter Canyon Diablo Sphere Impacting Cadmium.

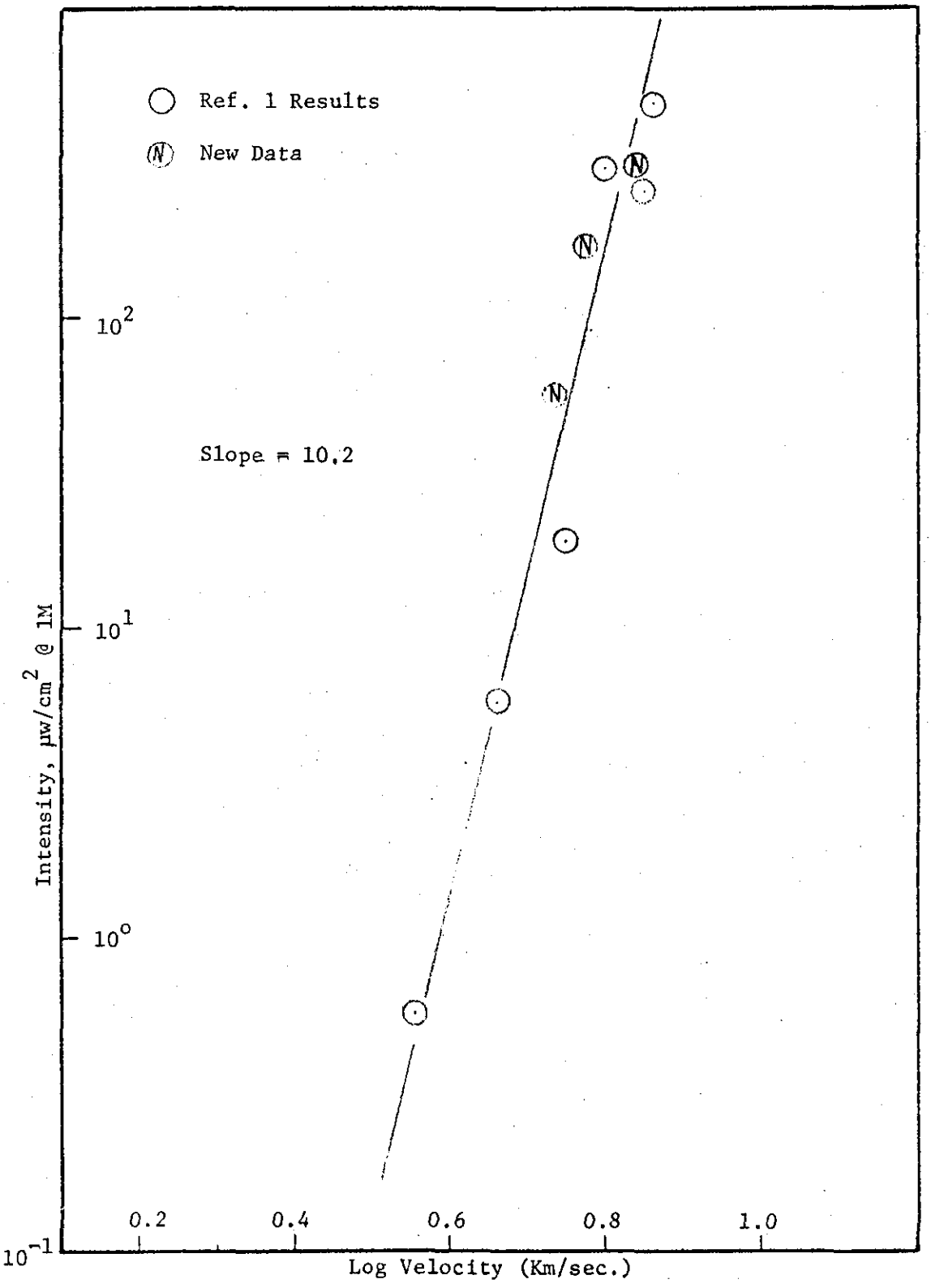

Figure 2. Spike Intensity Variation with Velocity at 3610Å for a 1.2 Millimeter Canyon Diablo Sphere Impacting Cadmium.

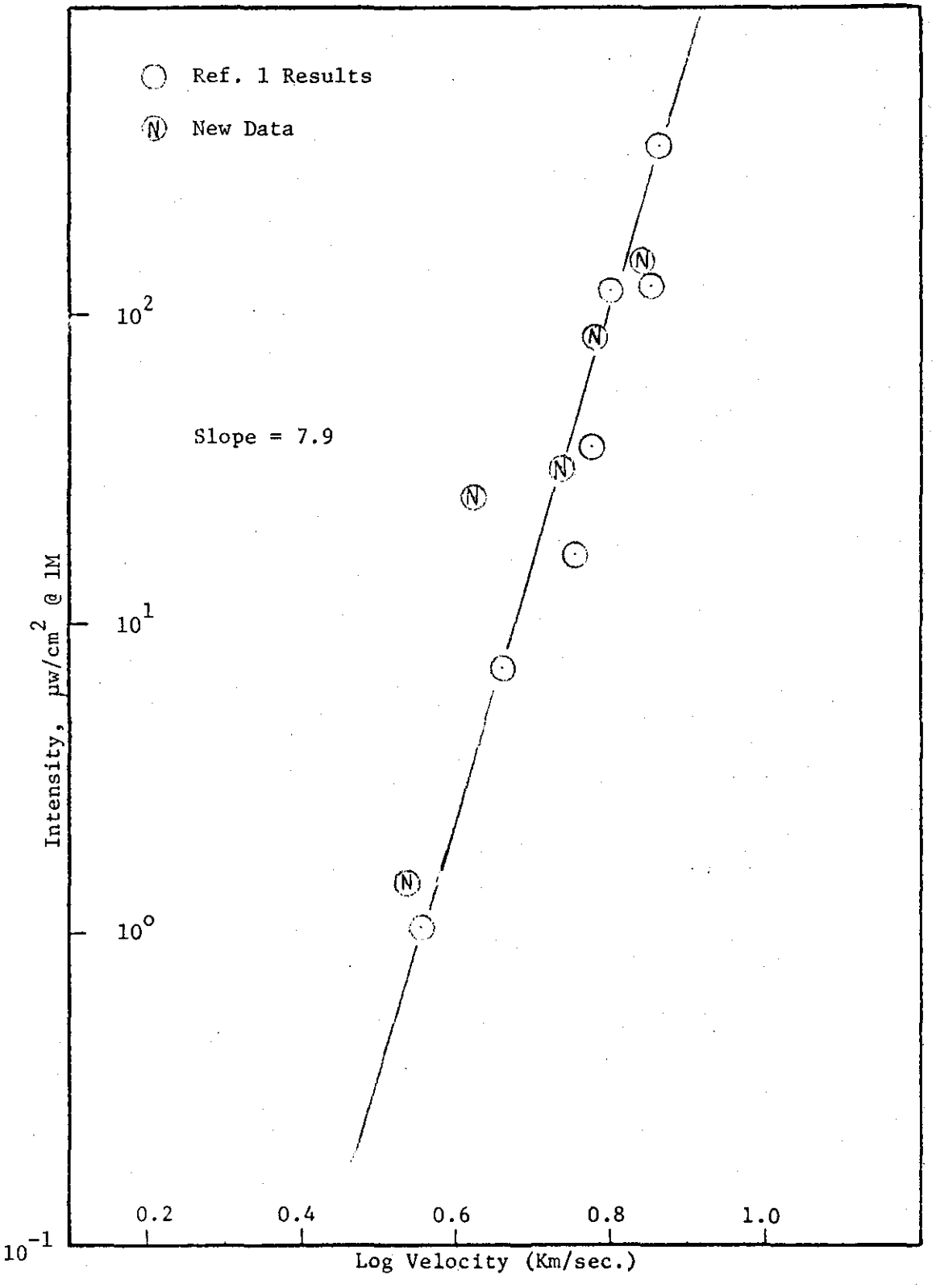

Figure 3. Spike Intensity Variation with Velocity at 4900Å for a 1.2 Millimeter Canyon Diablo Sphere Impacting Cadmium.

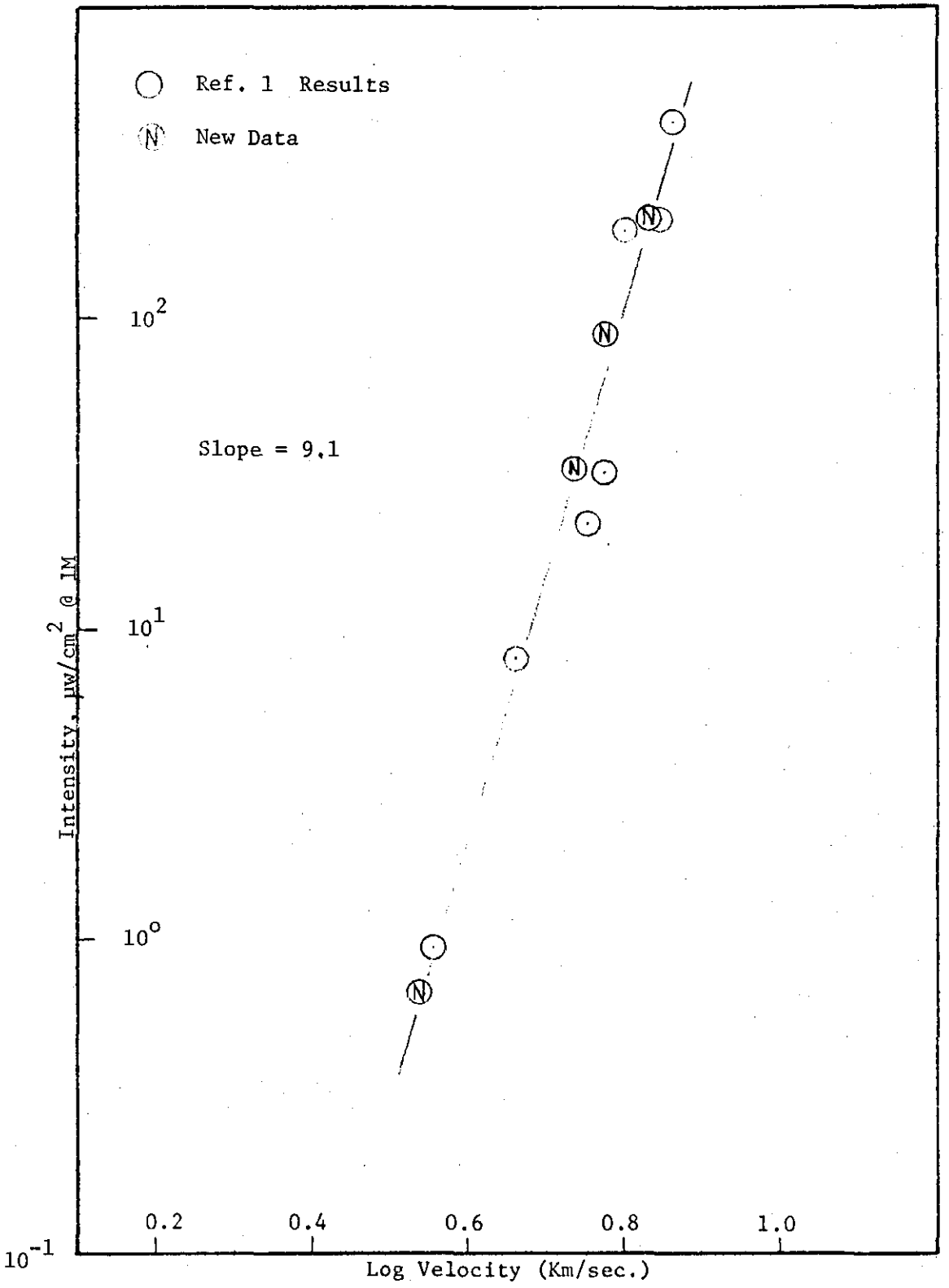

Figure 4. Spike Intensity Variation with Velocity at 5085Å for a 1.2 millimeter Canyon Diablo Sphere Impacting Cadmium.

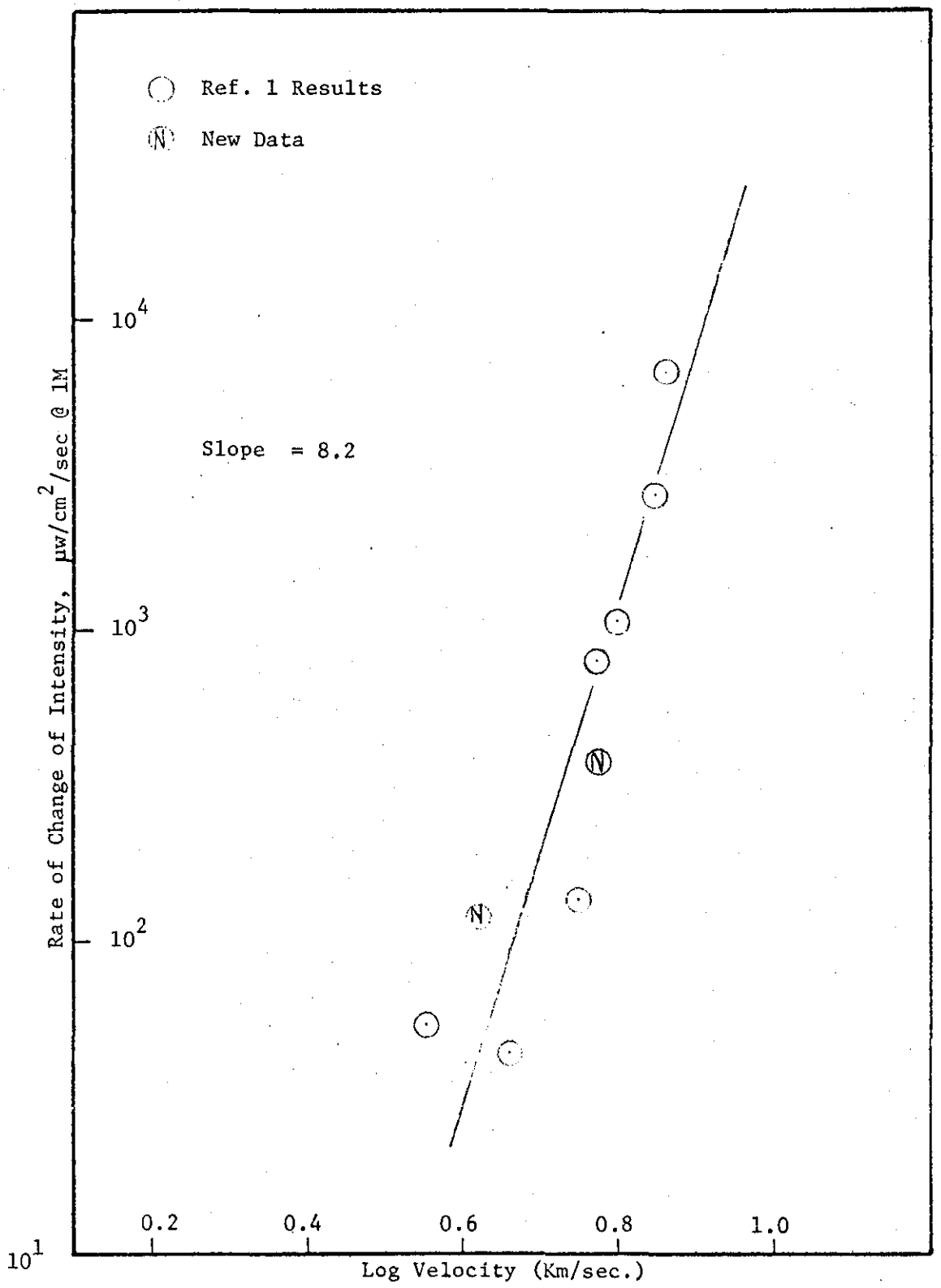

Figure 5. Rate of Change of Spike Intensity Variation with Velocity at 3261Å for a 1.2 Millimeter Canyon Diablo Sphere Impacting Cadmium.

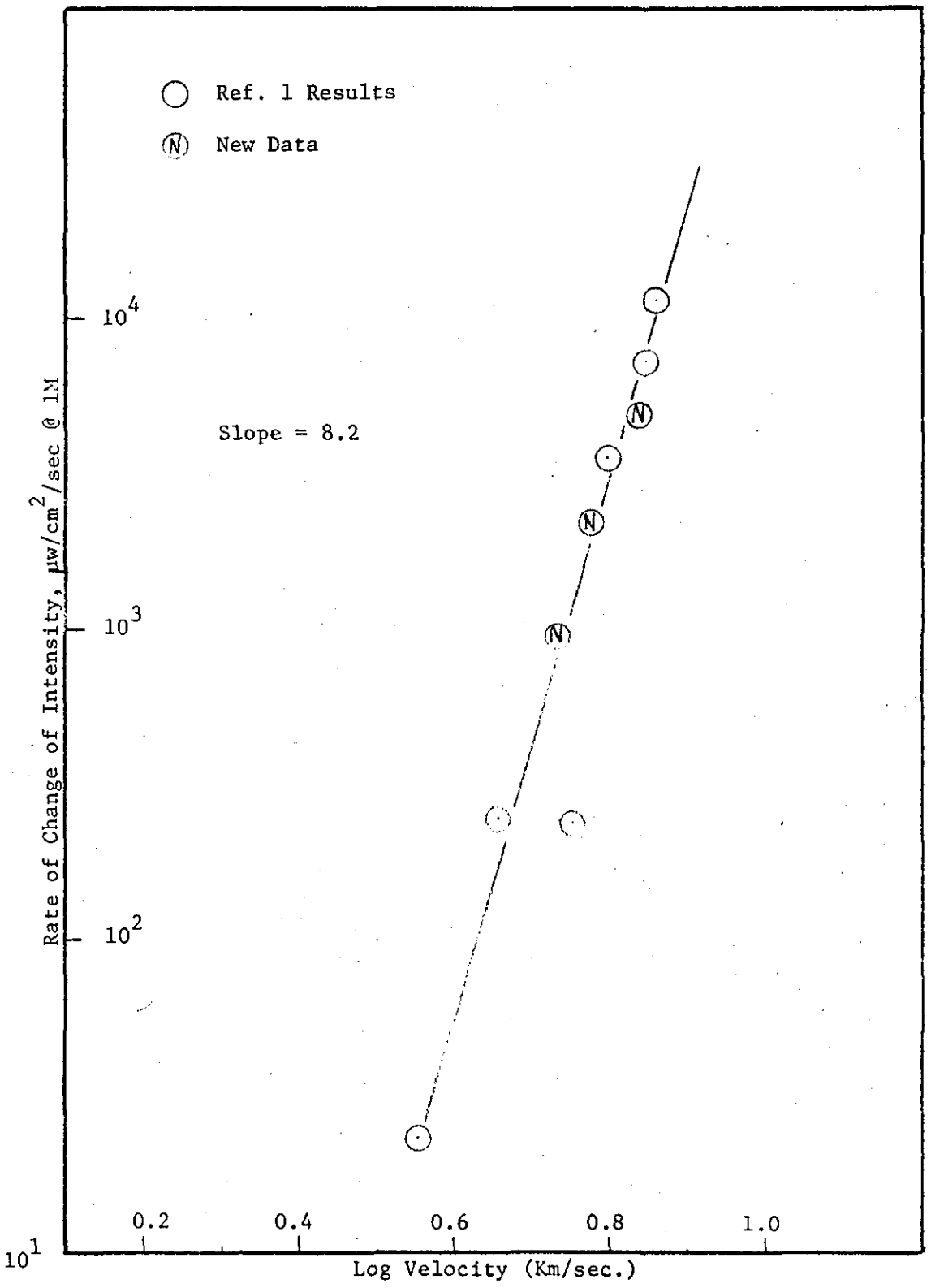

Figure 6. Rate of Change of Spike Intensity Variation with Velocity at 3610Å for a 1.2 Millimeter Canyon Diablo Sphere Impacting Cadmium.

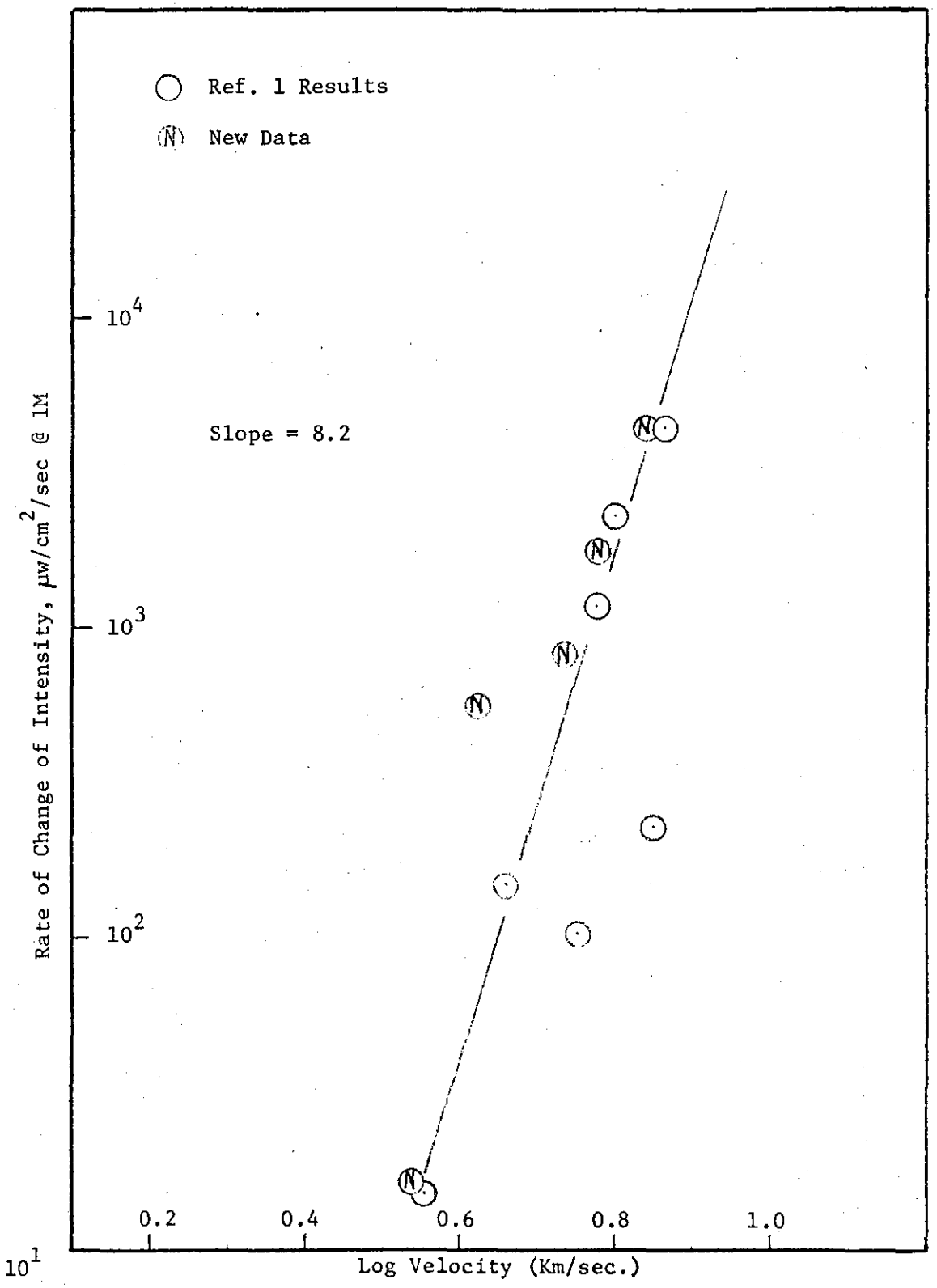

Figure 7. Rate of Change of Spike Intensity Variation with Velocity at 4900Å for a 1.2 Millimeter Canyon Diablo Sphere Impacting Cadmium.

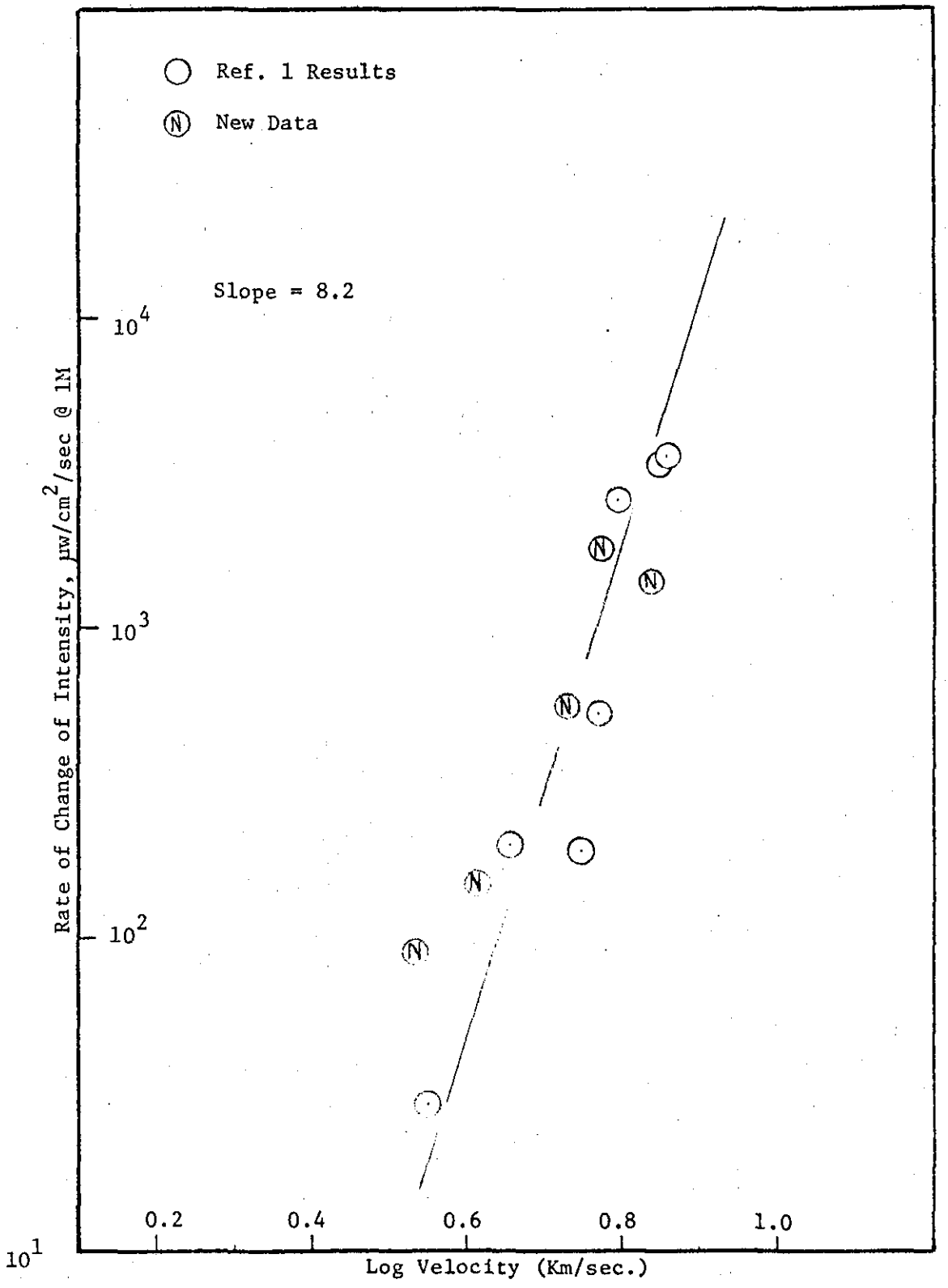

Figure 8. Rate of Change of Spike Intensity Variation with Velocity at 5085Å for a 1.2 Millimeter Canyon Diablo Sphere Impacting Cadmium.

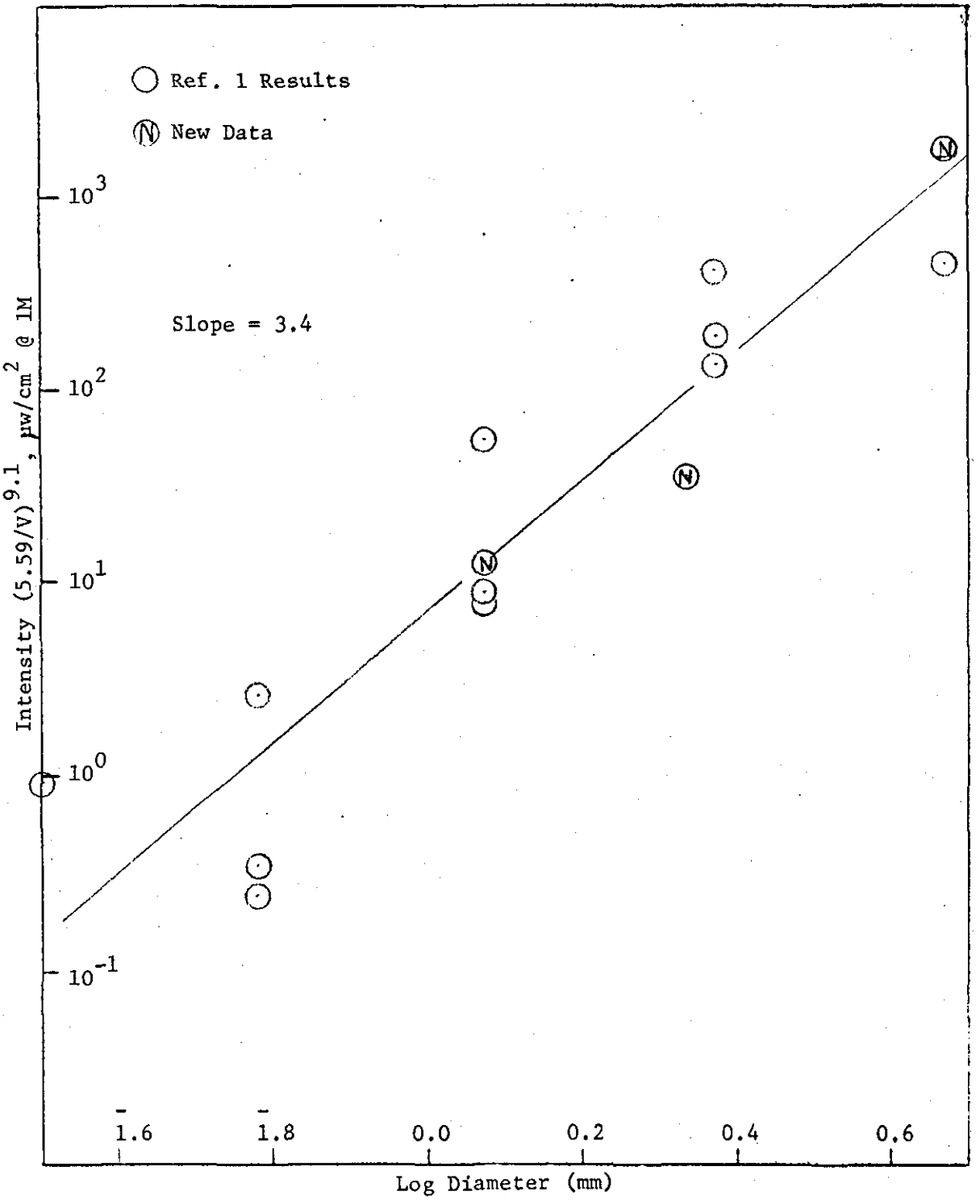

Figure 9. Dependence of Spike Intensity on Projectile Diameter at 3261Å for Canyon Diablo Impacting Cadmium.

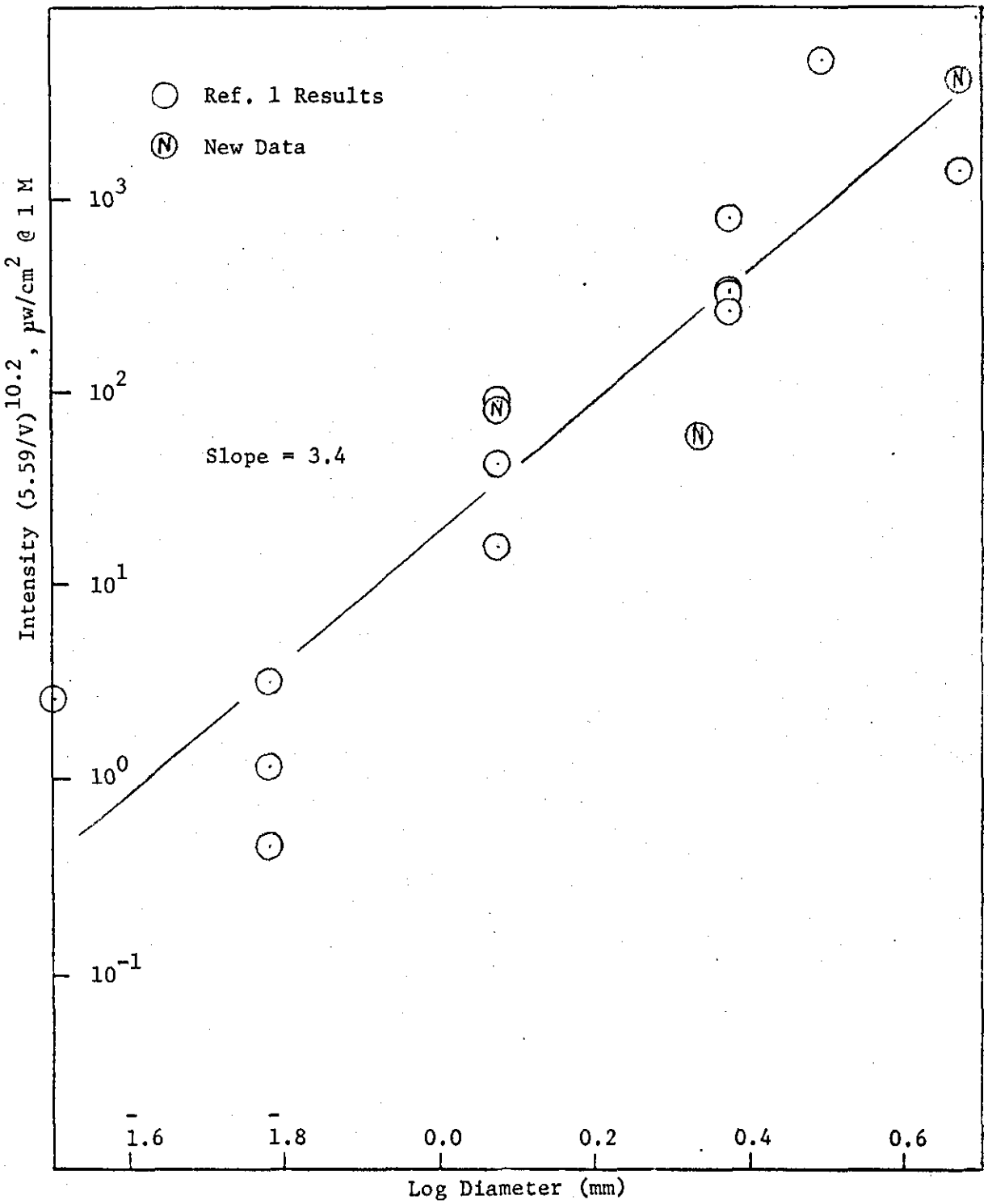

Figure 10. Dependence of Spike Intensity on Projectile Diameter at 3610Å for Canyon Diablo Impacting Cadmium.

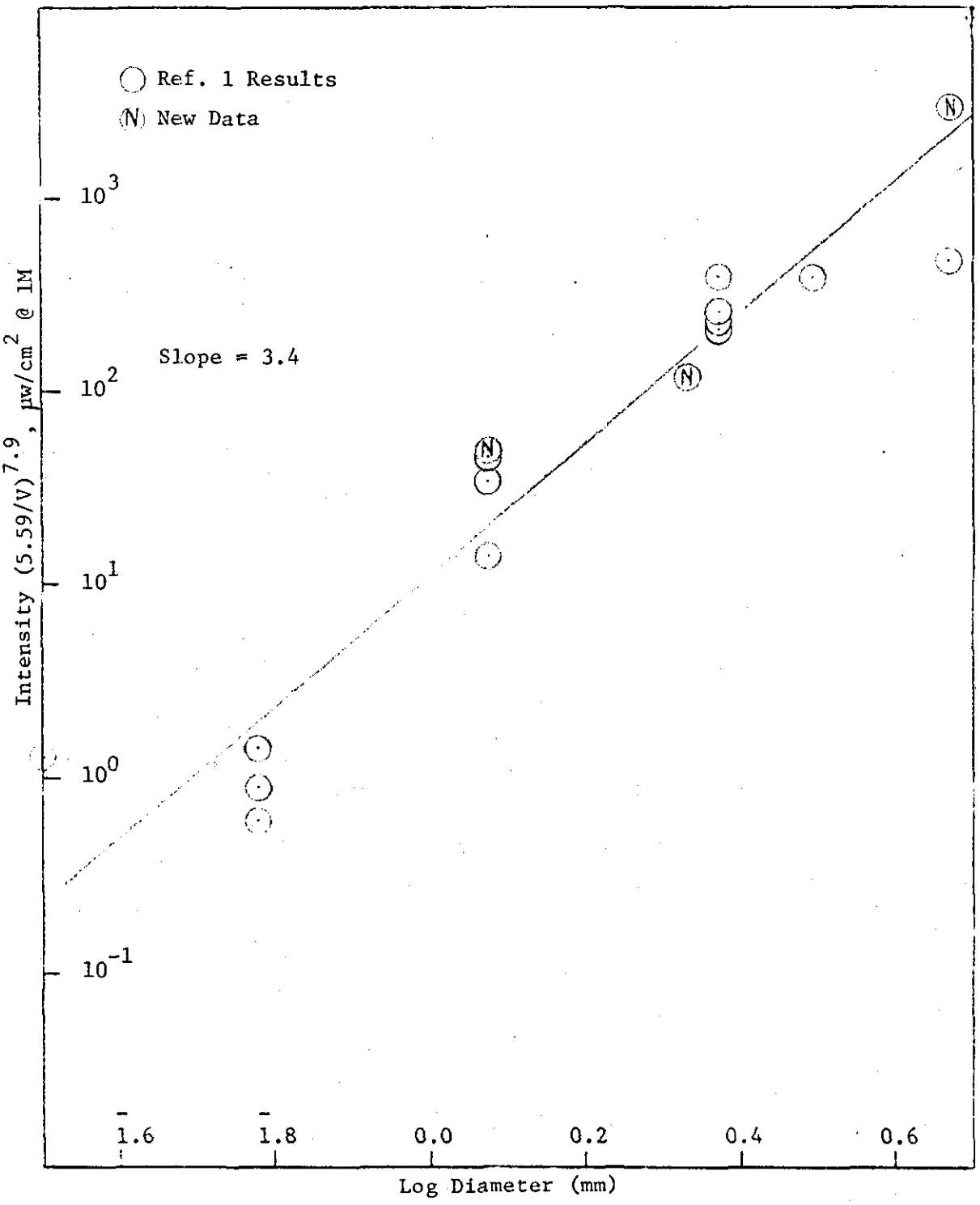

Figure 11. Dependence of Spike Intensity on Projectile Diameter at 4900Å for Canyon Diablo Impacting Cadmium.

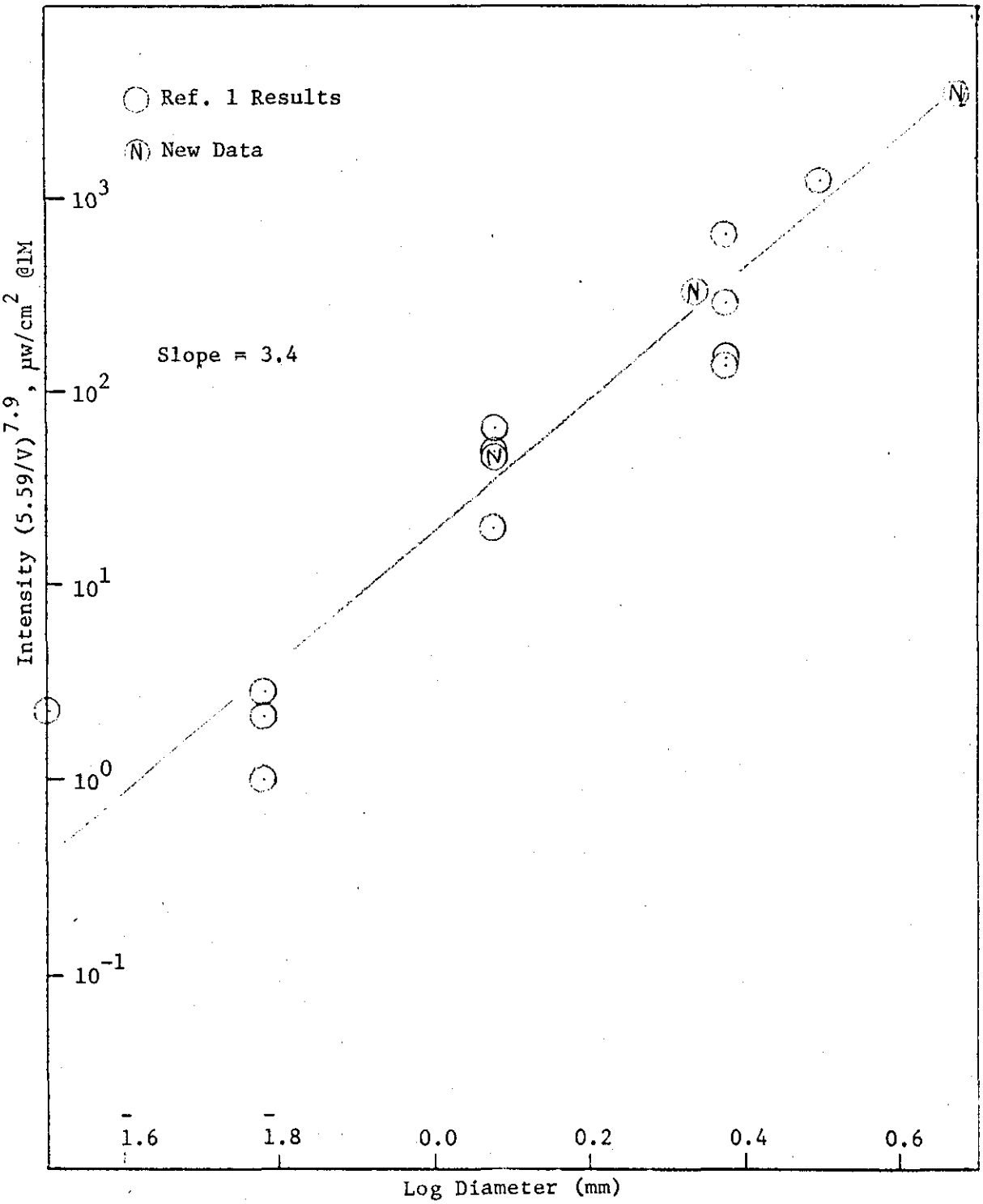

Figure 12. Dependence of Spike Intensity on Projectile Diameter at 5085Å for Canyon Diablo Impacting Cadmium.

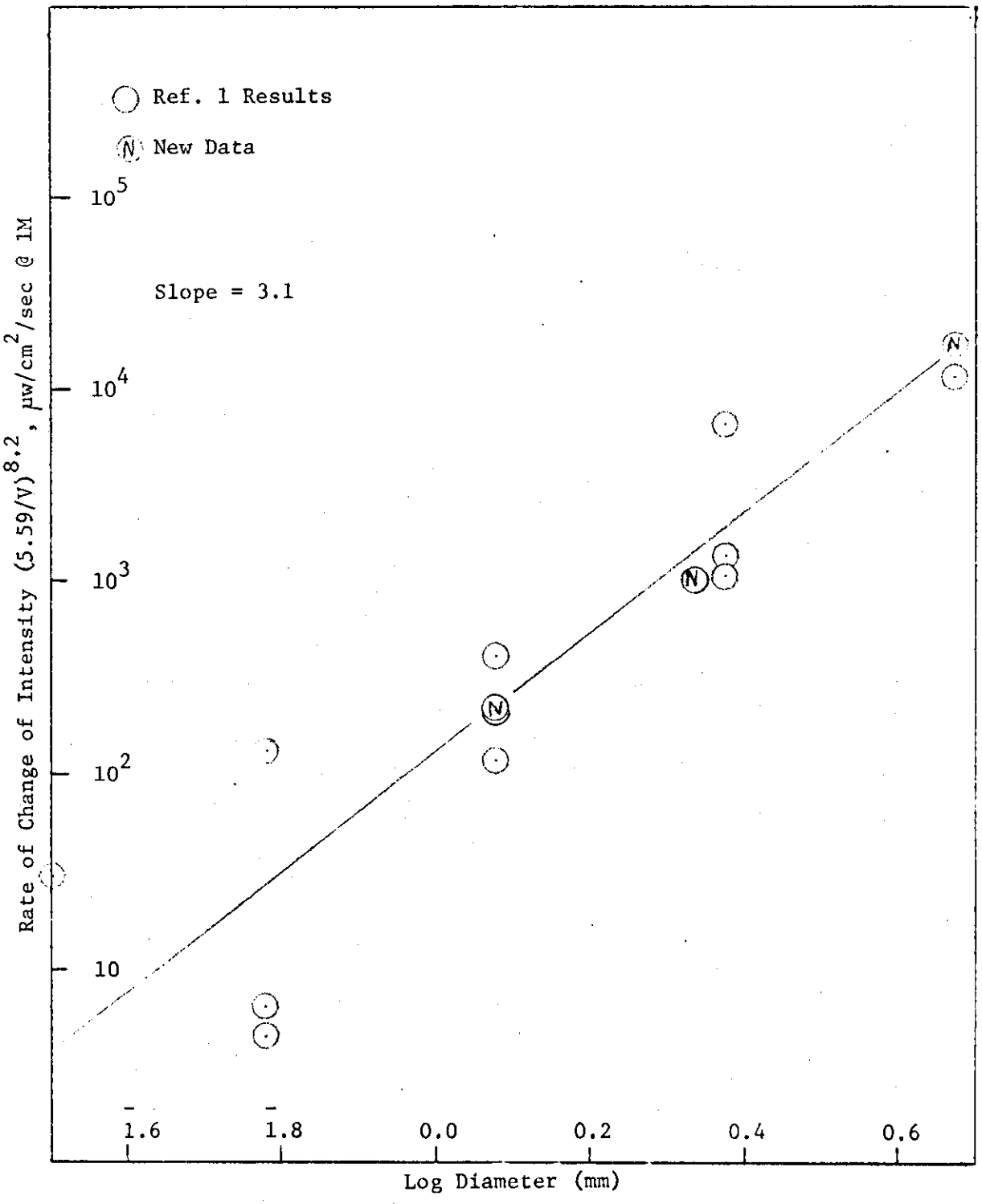

Figure 13. Dependence of Spike Rate of Change of Intensity on Projectile Diameter at 3261Å for Canyon Diablo Impacting Cadmium.

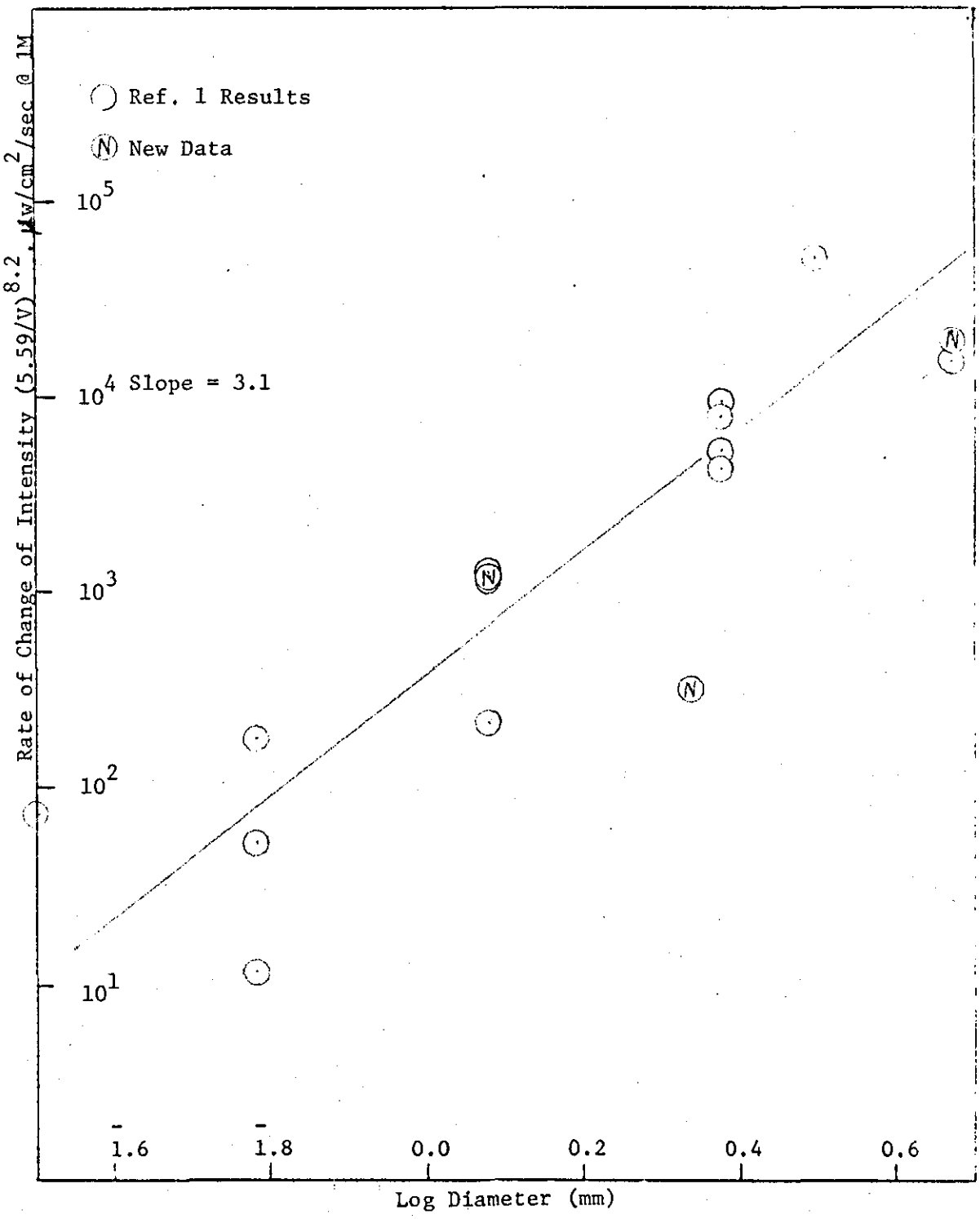

Figure 14. Dependence of Spike Rate of Change of Intensity on Projectile Diameter at 3610Å for Canyon Diable Impacting Cadmium.

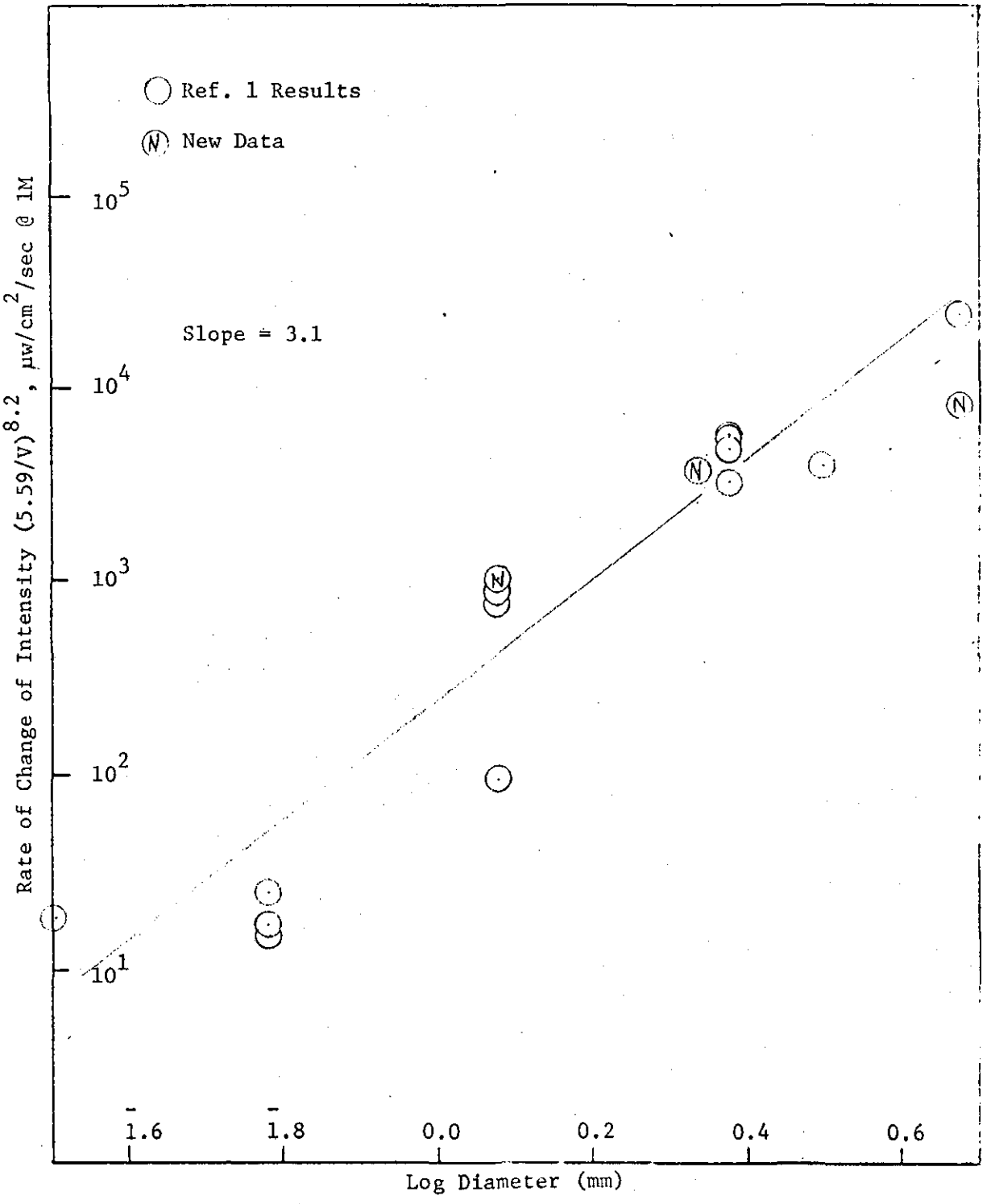

Figure 15. Dependence of Spike Rate of Change of Intensity on Projectile Diameter at 4900Å for Canyon Diablo Impacting Cadmium.

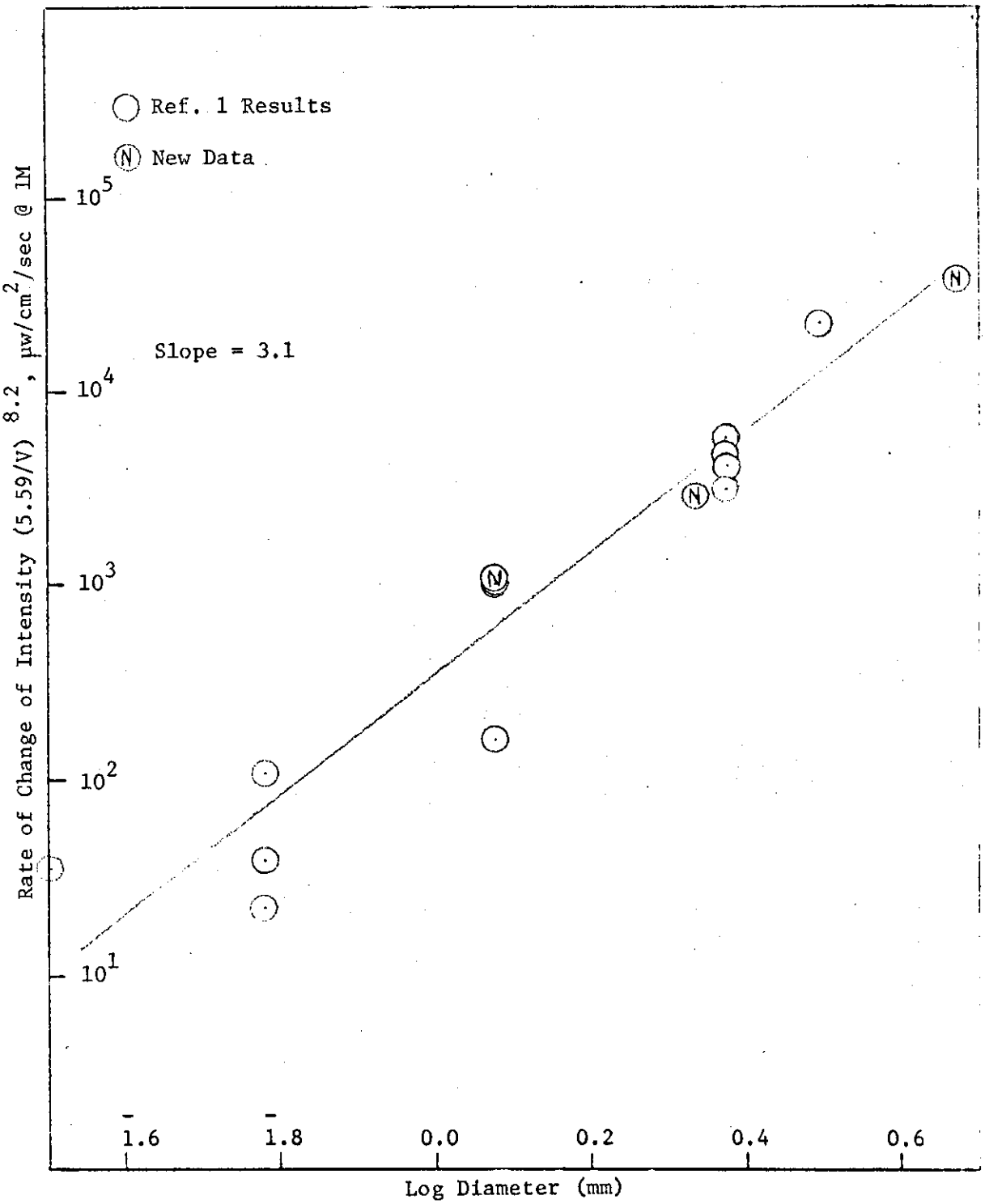

Figure 16. Dependence of Spike Rate of Change of Intensity on Projectile Diameter at 5085Å for Canyon Diablo Impacting Cadmium.

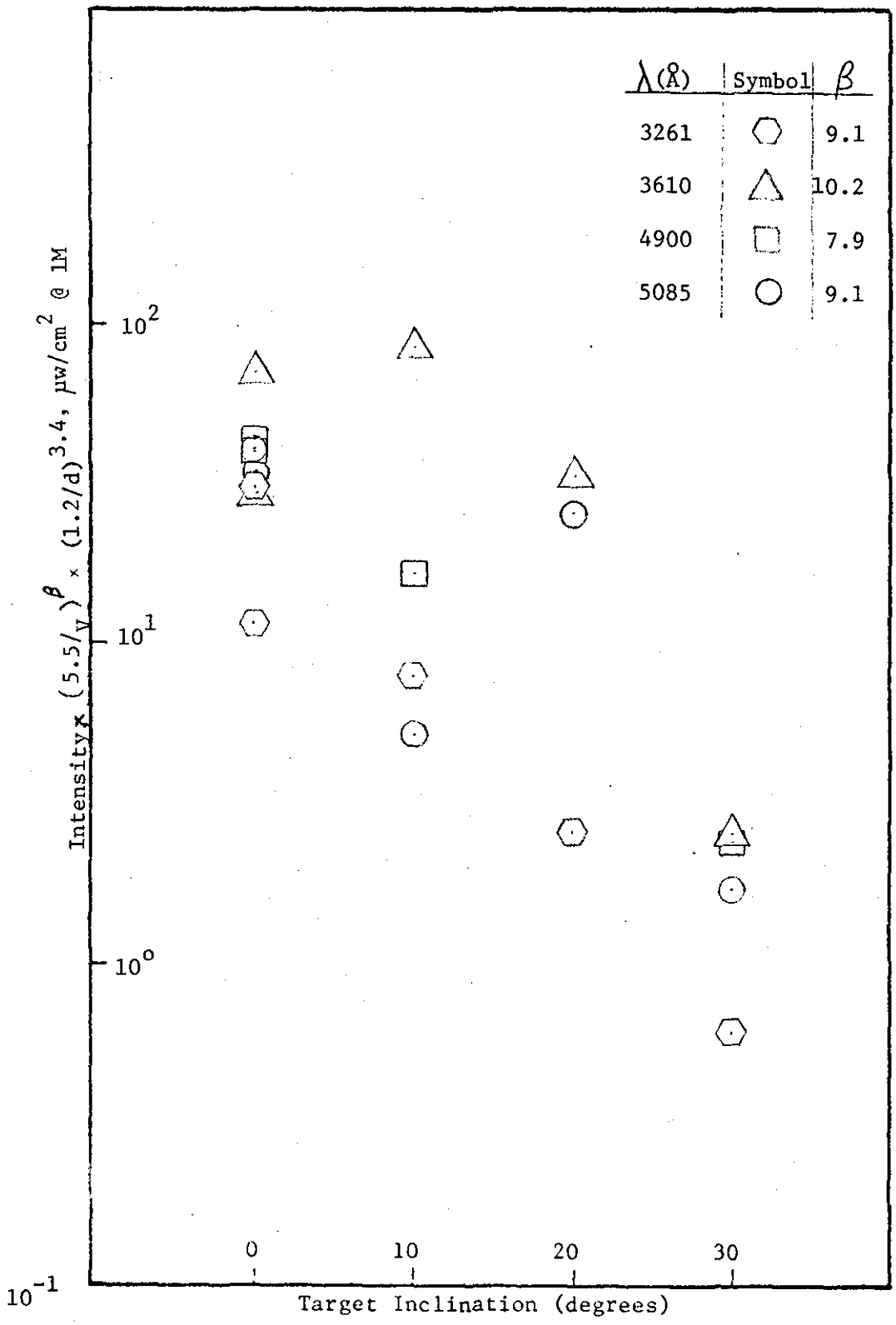

Figure 17. Influence of Target Orientation on Spike Intensity.

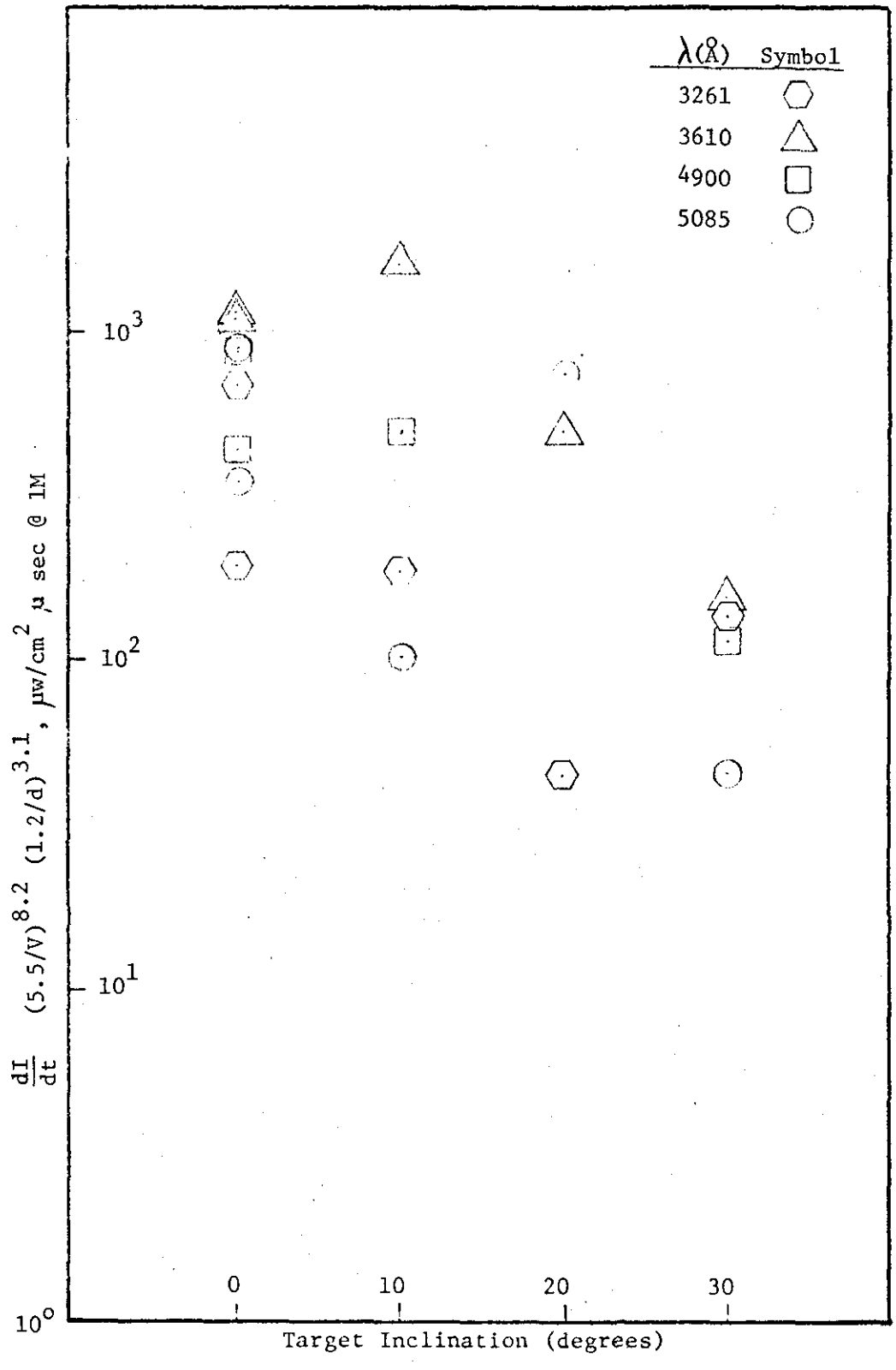

Figure 18. Influence of Target Orientation on Rate of Change of Flash Intensity.

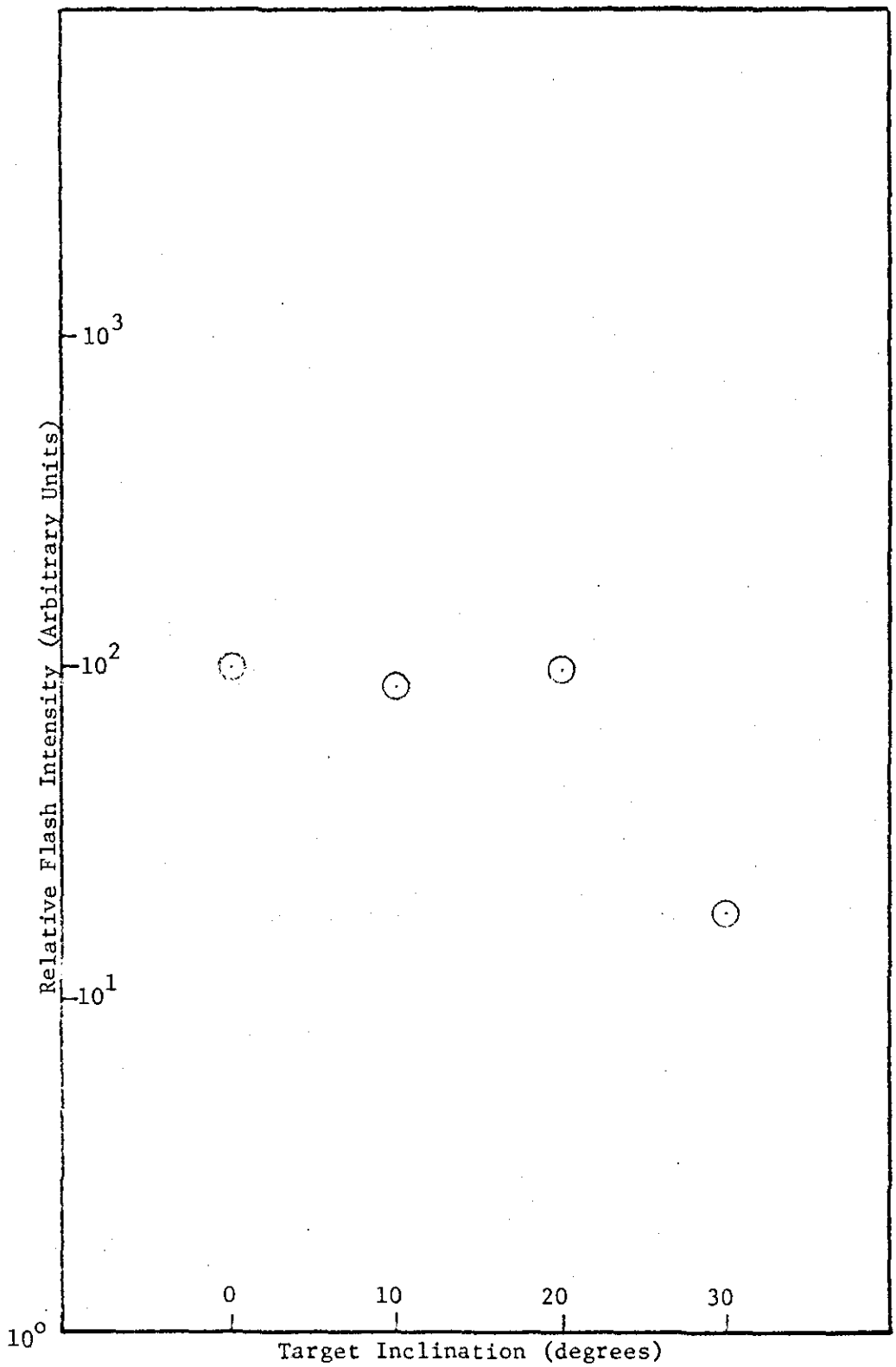

Figure 19. Influence of Target Orientation on Average Flash Intensity Normalized to the Velocity Normal.

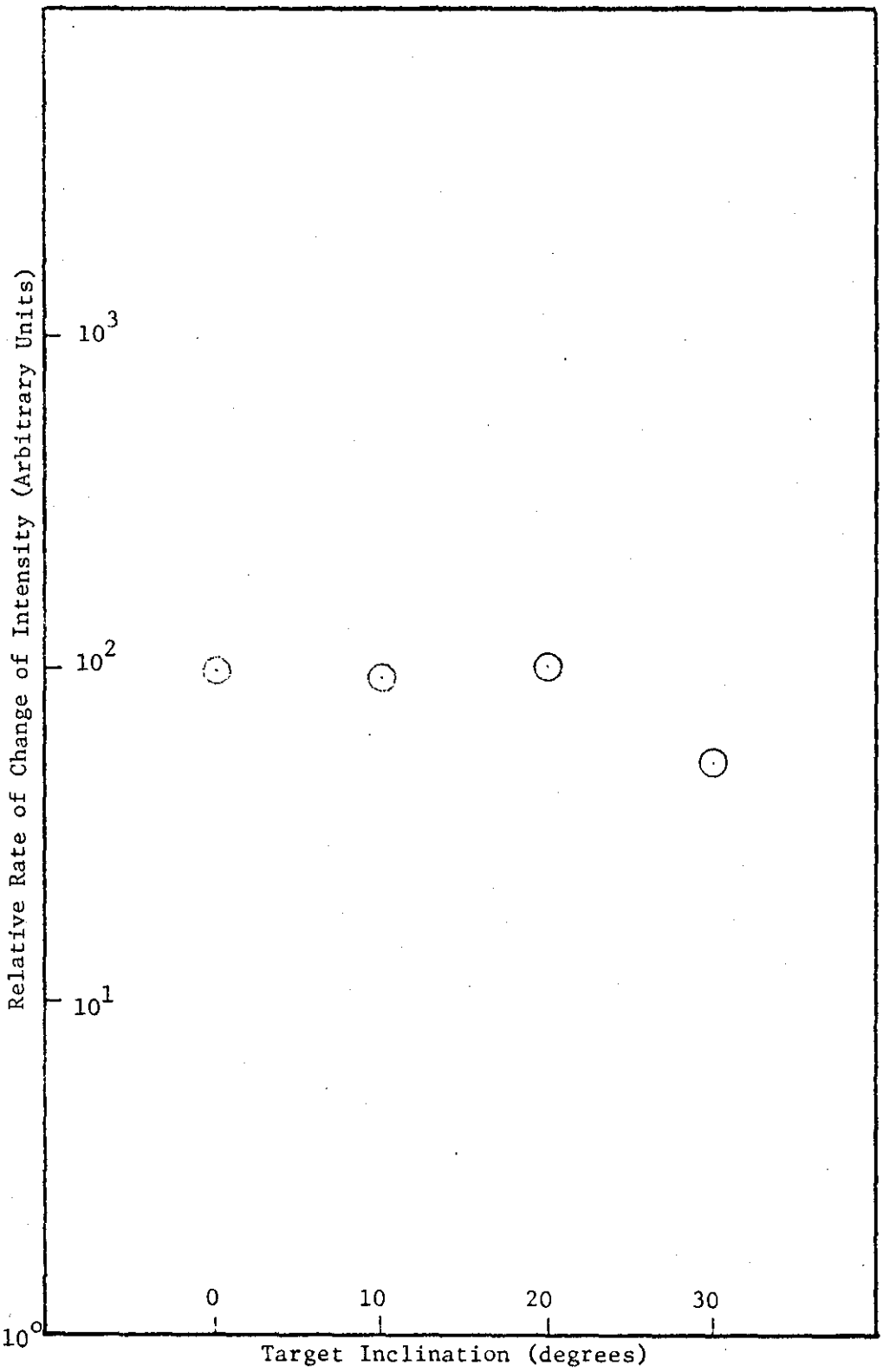

Figure 20. Influence of Target Orientation on Average Flash Rate of Change of Intensity Normalized to the Velocity Normal.

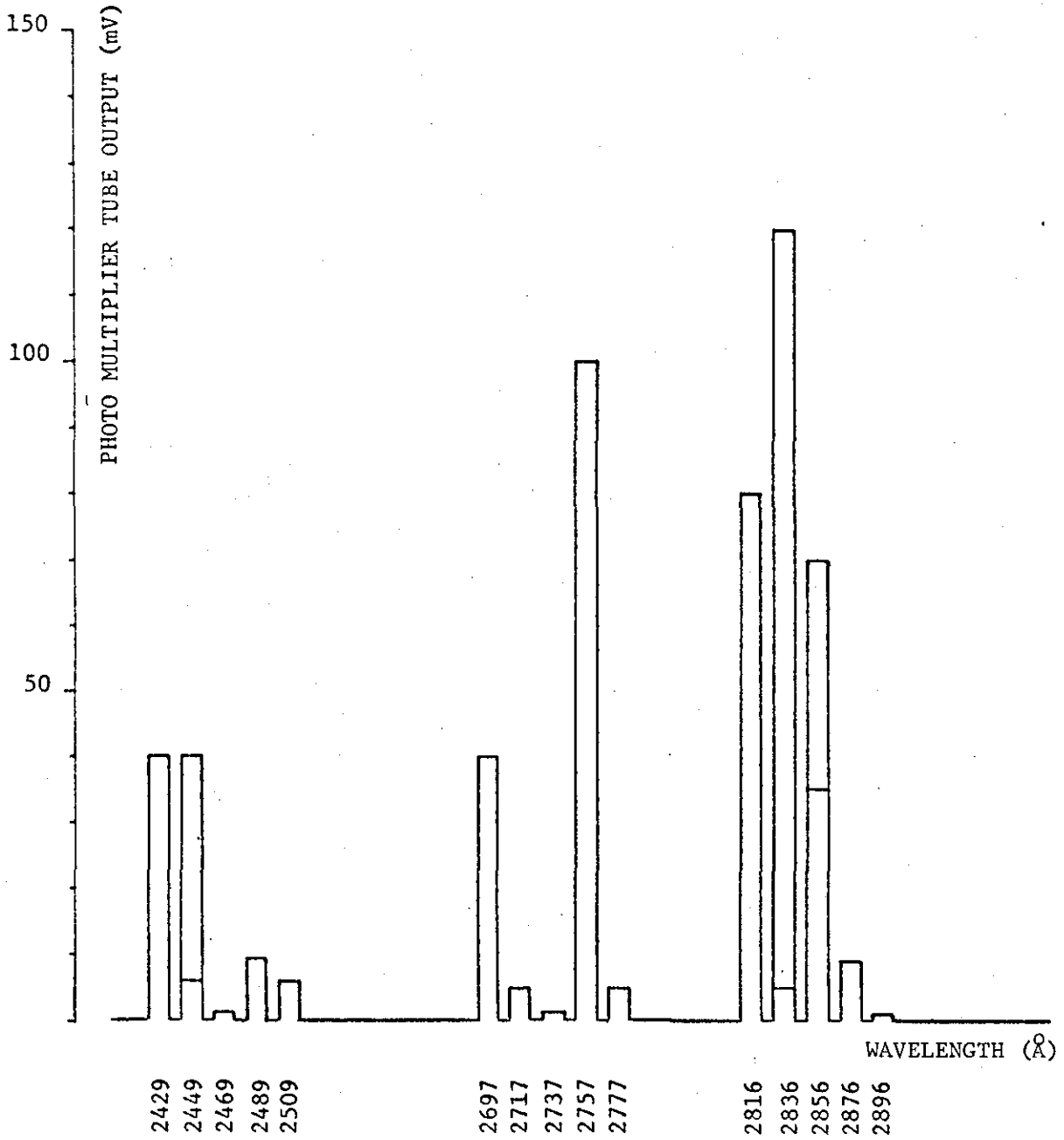

Figure 21. Spectral Distribution of Radiation in the Bandwidth of 3 Filters for Copper Impacting Cadmium.

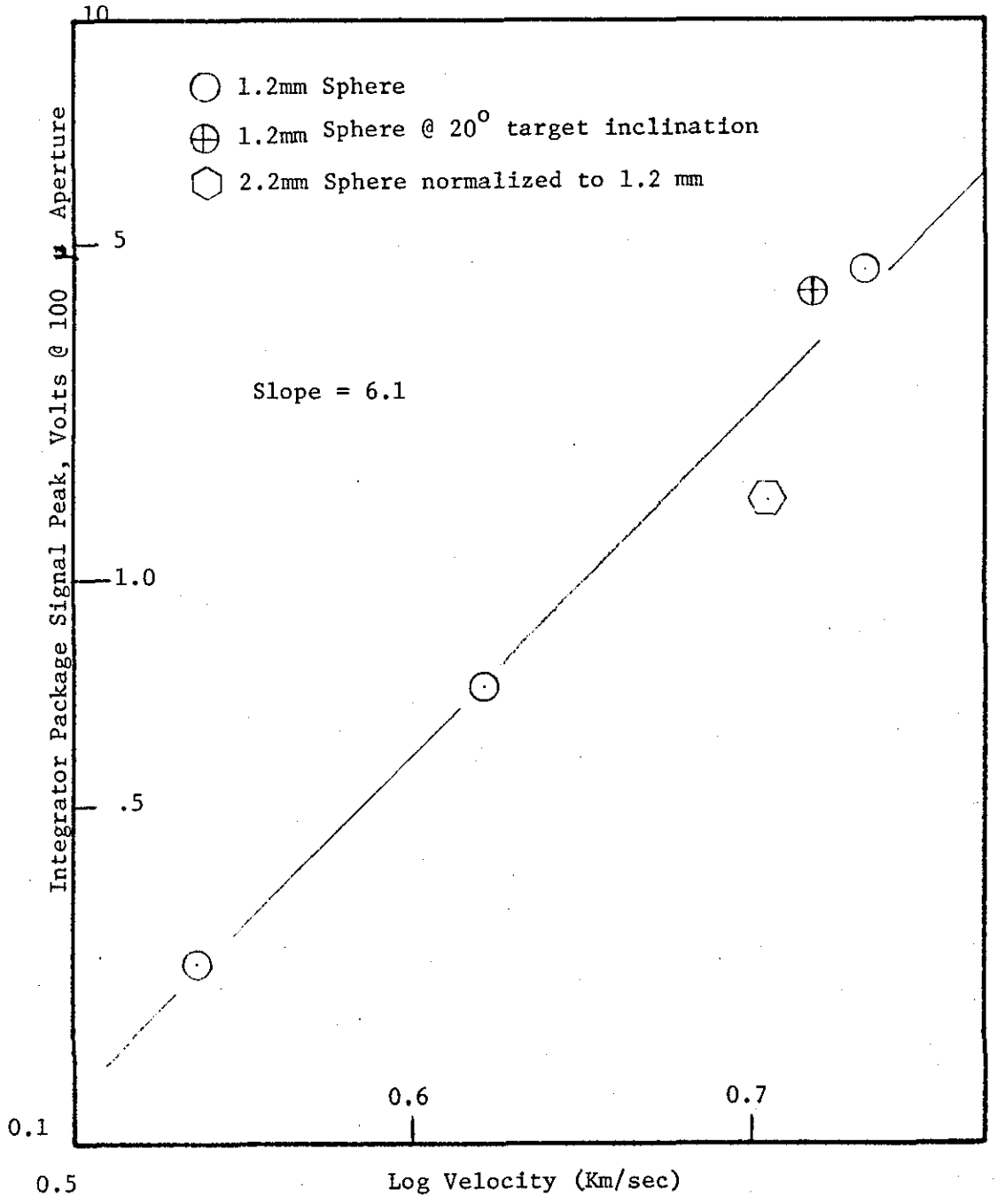

Figure 22. Variation of Integrator Signal Peak with Projectile Velocity at 3735Å for Canyon Diablo Spheres Impacting Cadmium.

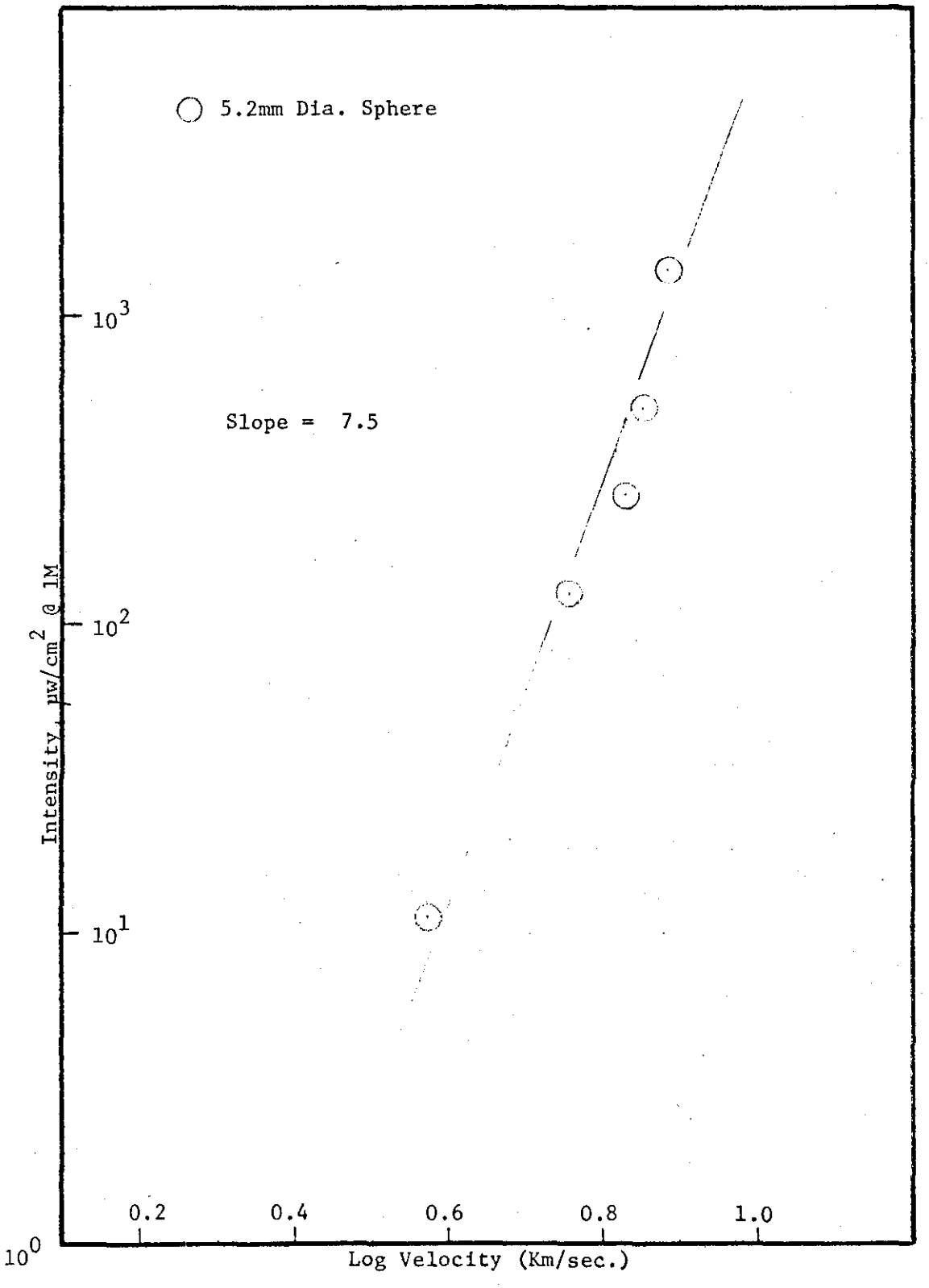

Figure 23. Spike Intensity Variation with Velocity at 3261Å for a Mg/Li Projectile Impacting Cadmium.

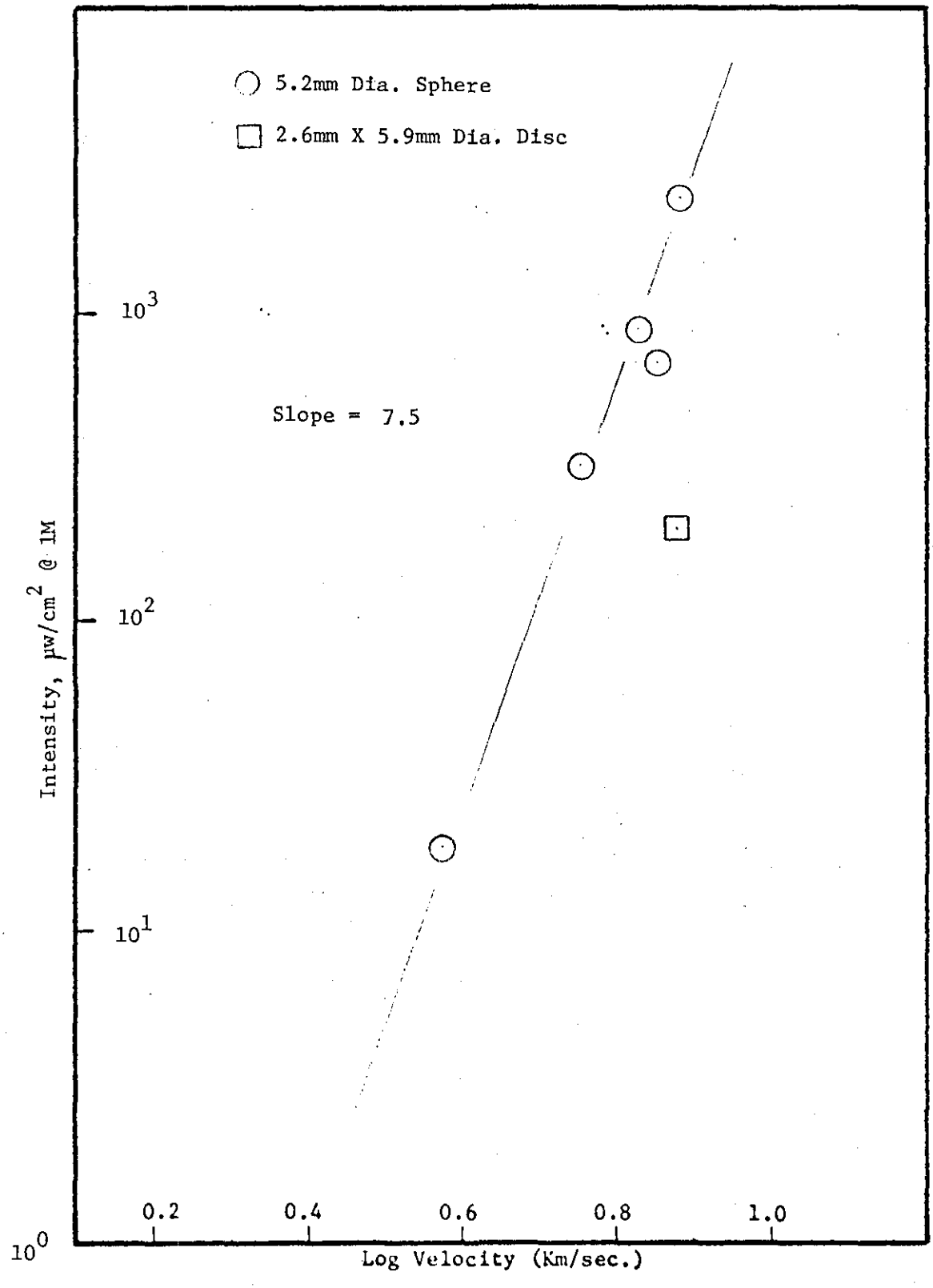

Figure 24. Spike Intensity Variation with Velocity at 3610Å for a Mg/Li Projectile Impacting Cadmium.

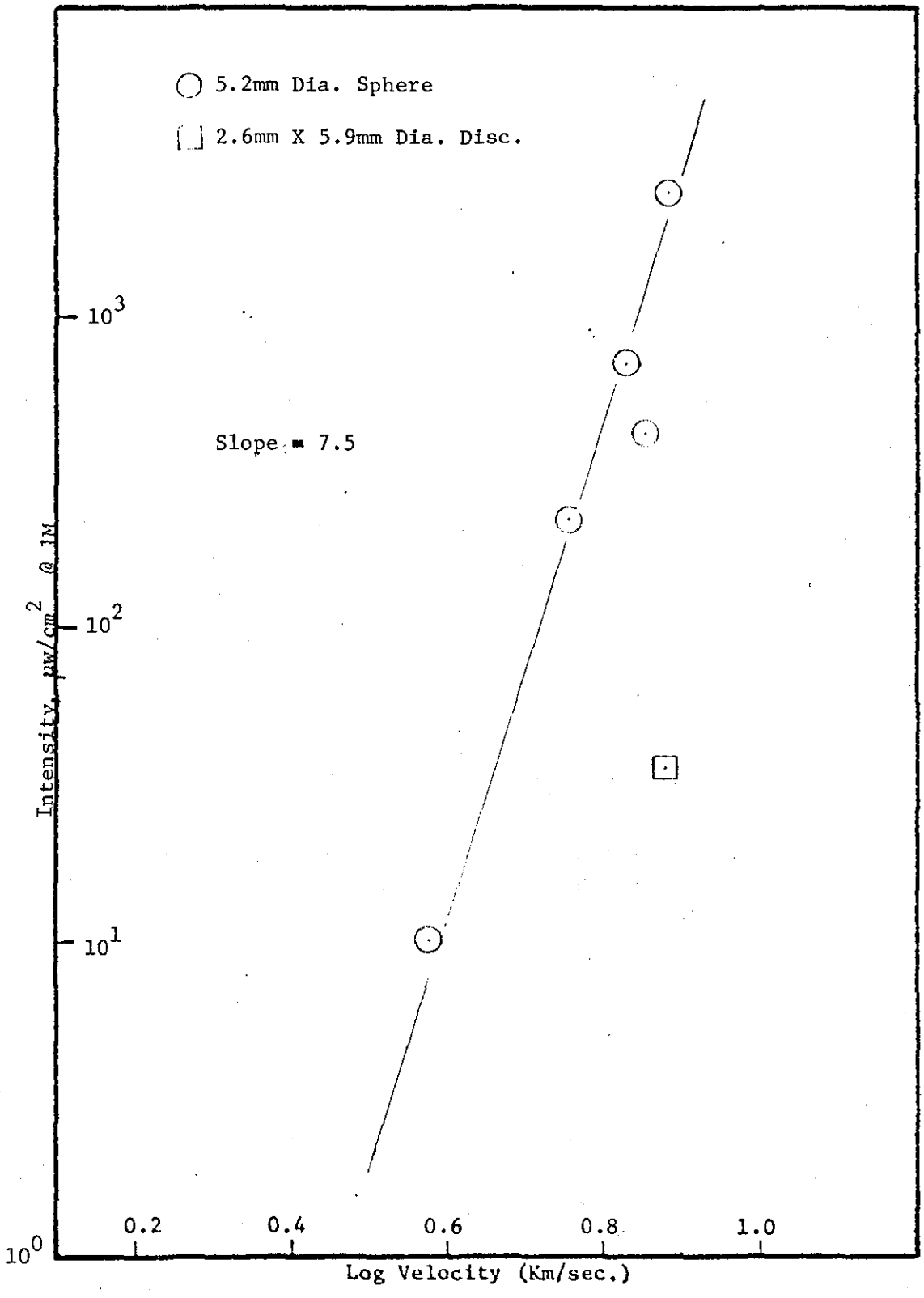

Figure 25. Spike Intensity Variation with Velocity at 4900Å for a Mg/Li Projectile Impacting Cadmium.

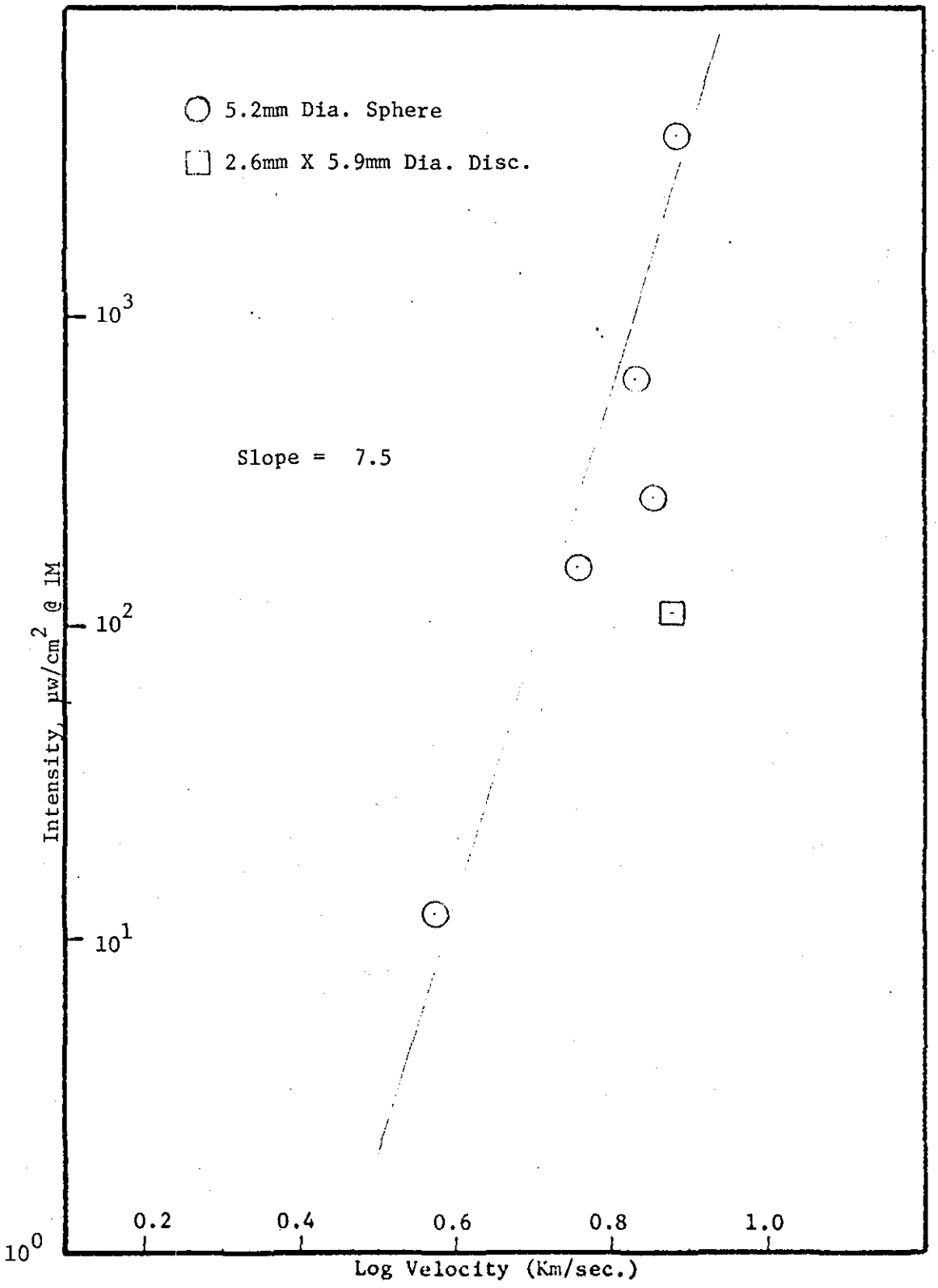

Figure 26. Spike Intensity Variation with Velocity at 5085Å for a Mg/Li Projectile Impacting Cadmium.

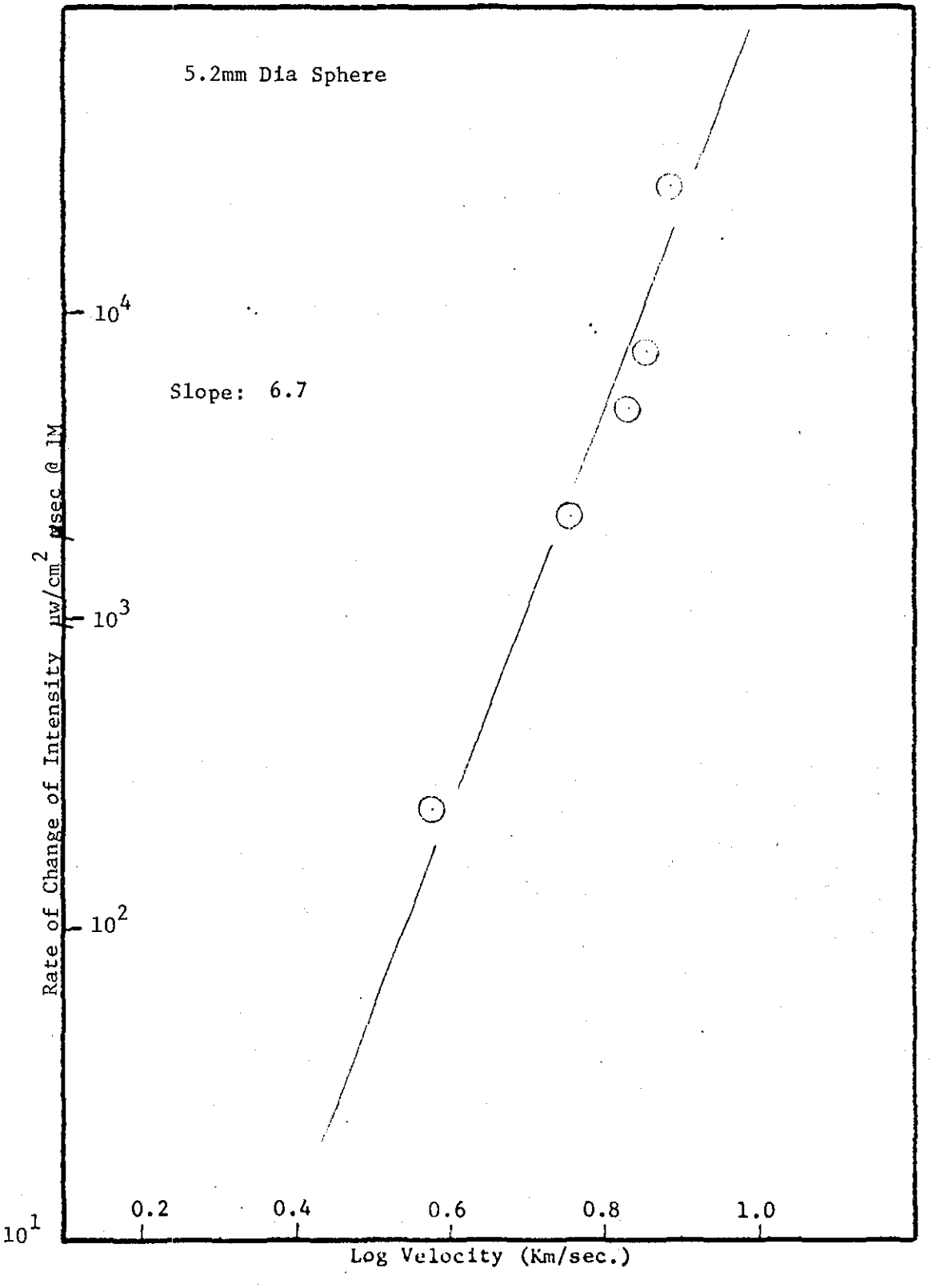

Figure 27. Variation of Rate of Change of Spike Intensity with Velocity at 3261Å for a Mg/Li Projectile Impacting Cadmium.

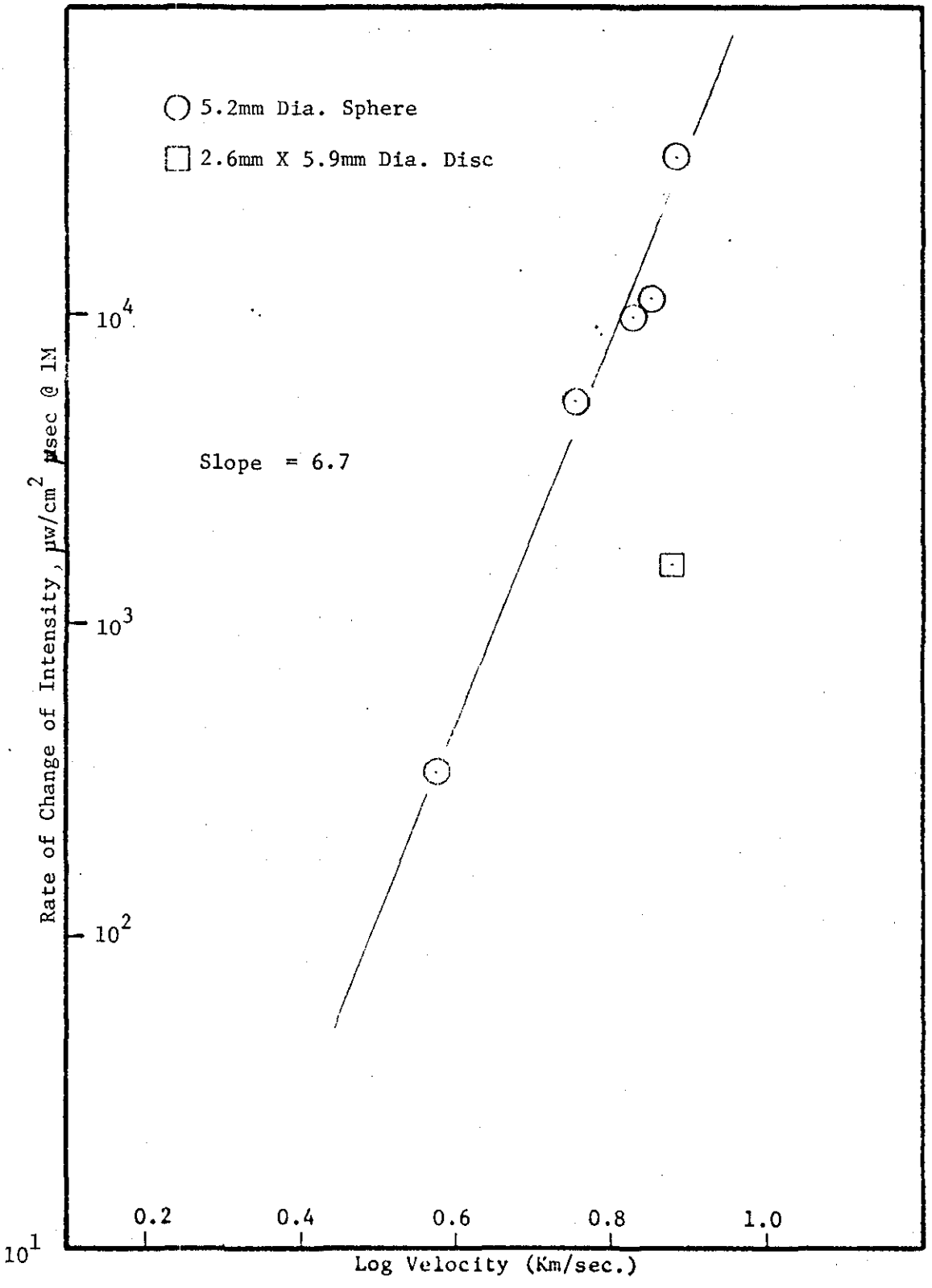

Figure 28. Variation of Rate of Change of Spike Intensity with Velocity at 3610Å for a Mg/Li Projectile Impacting Cadmium.

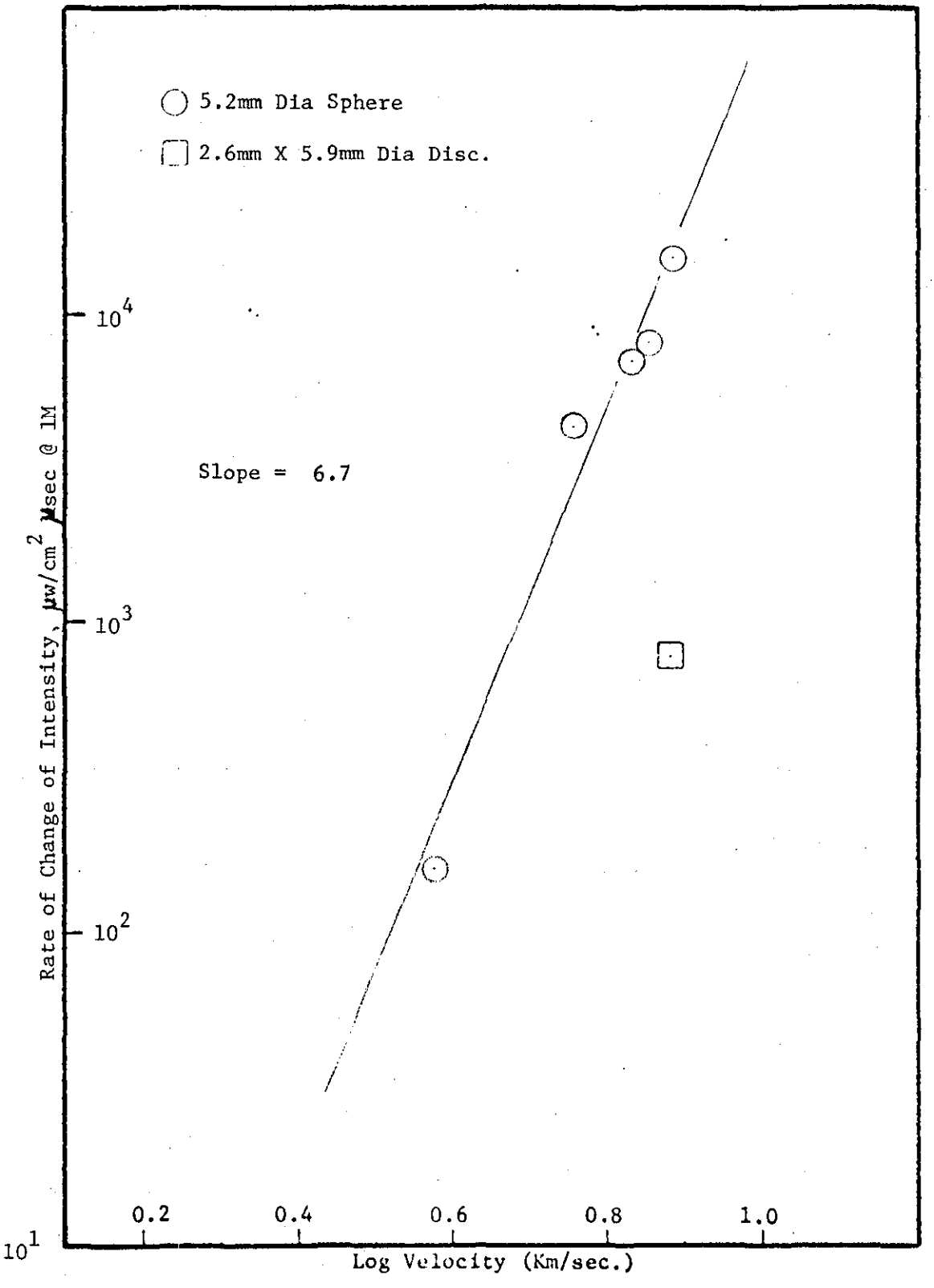

Figure 29. Variation of Rate of Change of Spike Intensity with Velocity at 4900Å for a Mg/Li Projectile Impacting Cadmium.

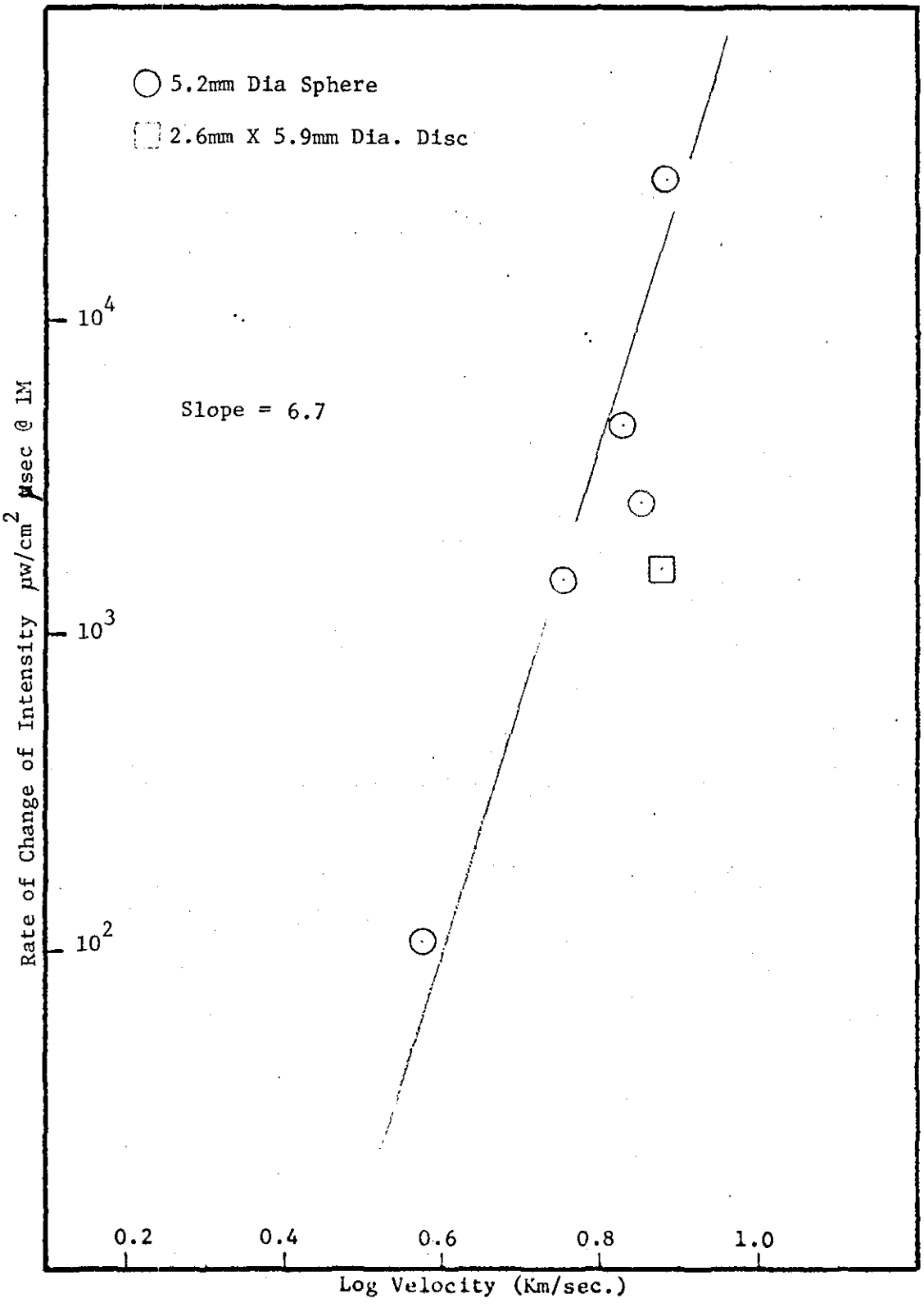

Figure 30. Variation of Rate of Change of Spike Intensity with Velocity at 5085Å for a Mg/Li Projectile Impacting Cadmium.

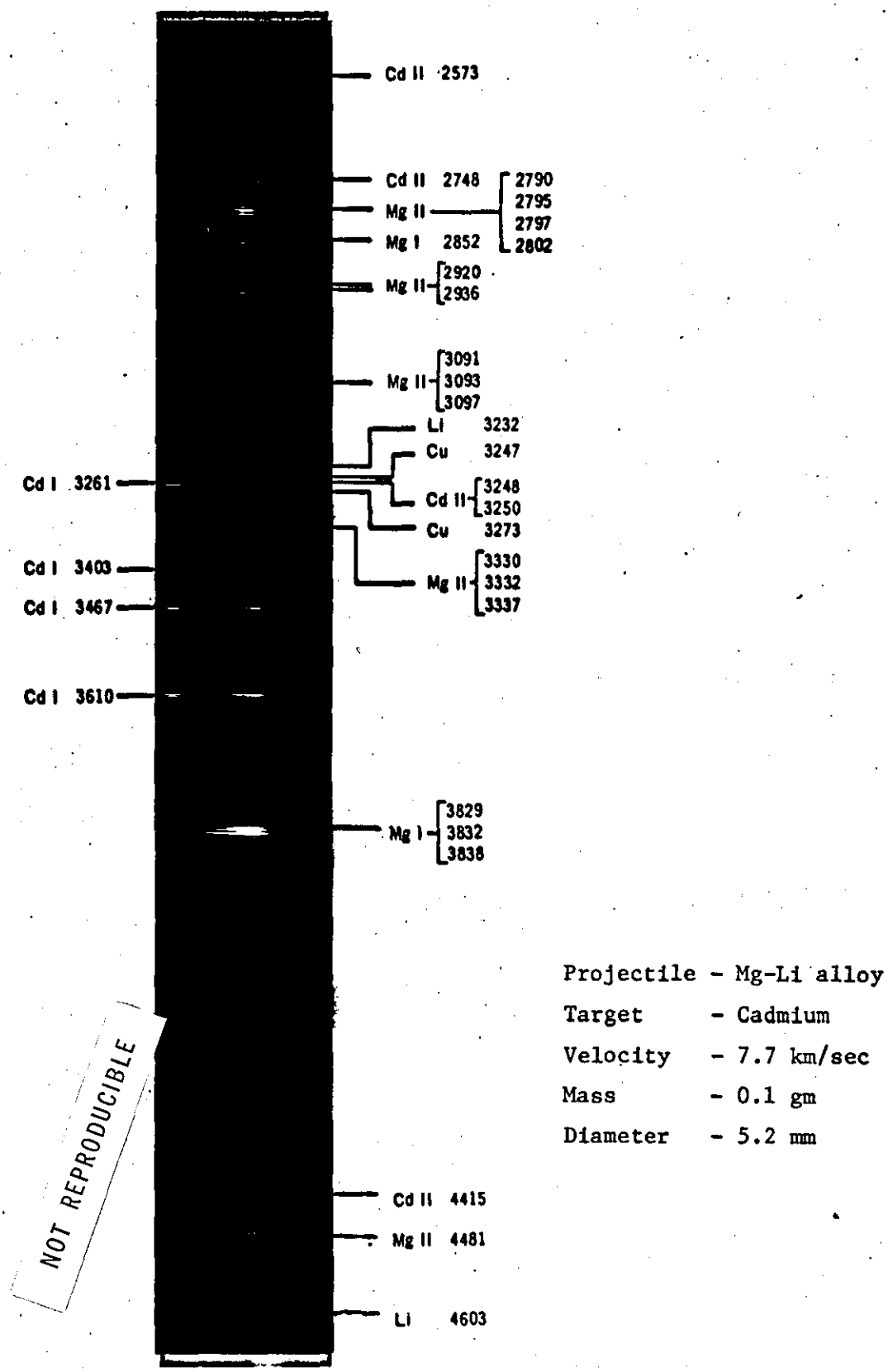

Figure 31. Spectrogram of the Flash Produced by the Impact of a Mg Li Projectile on a Cadmium Target

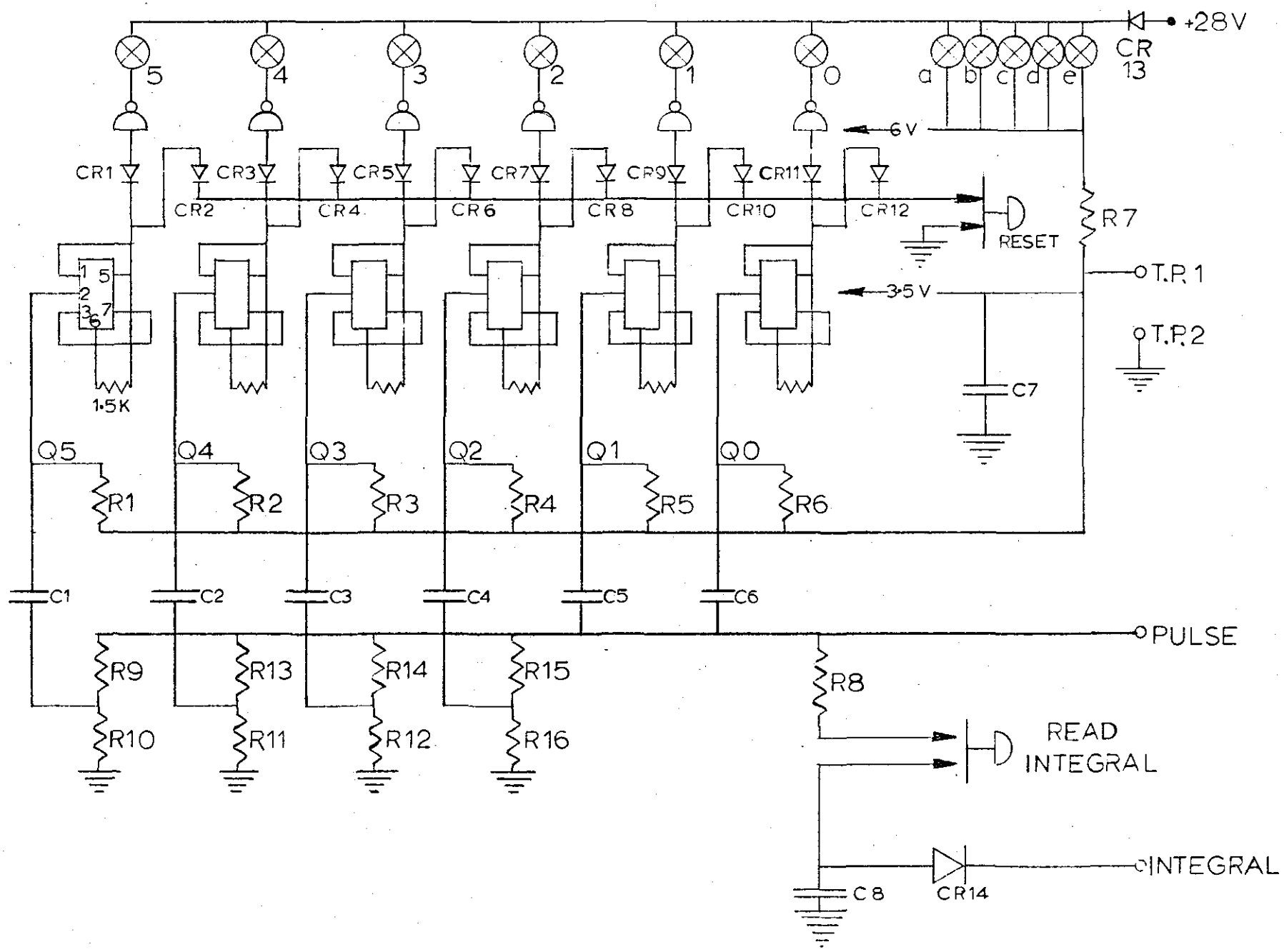

FIGURE 32. PEAK DETECTOR-QUANTIZER CIRCUIT

PEAK DETECTOR - QUANTIZER CIRCUIT

SYMBOL	VALUE
R1 - R5	3.3K
R6	22K
R7	15 (1W)
R8	180
R9 - R12	82
R13	120
R14	150
R15	180
R16	56
C1 - C6	0.01 μf 200 V
C7	240 μf 6 V
C8	47 μf 35 V
CR1 - CR12	SG 22
CR13	LRR 200-426 SEMCOR
CR14	FJT 1000 - SELECTED FOR LOW LEAKAGE

LEGEND FOR FIGURE 32.

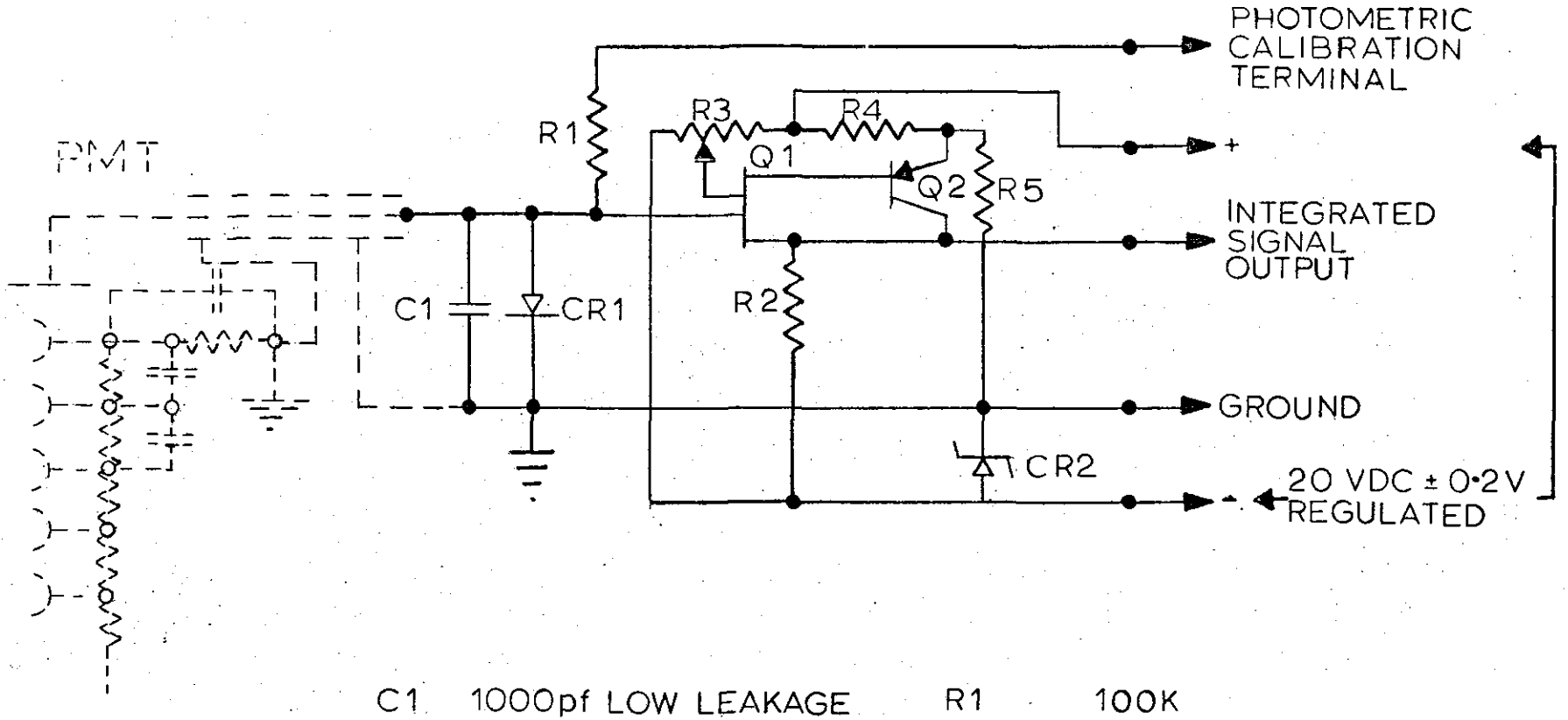

C1	1000pf LOW LEAKAGE	R1	100K
CR1	FCH FJT 1000	R2	3·3 K
CR2	IN 3016B ZENER DIODE	R3	50 K POT.
Q1	MFE 3007	R4	220 W
Q2	2N 2907A	R5	1 K

FIGURE 33. INTEGRATOR CIRCUIT

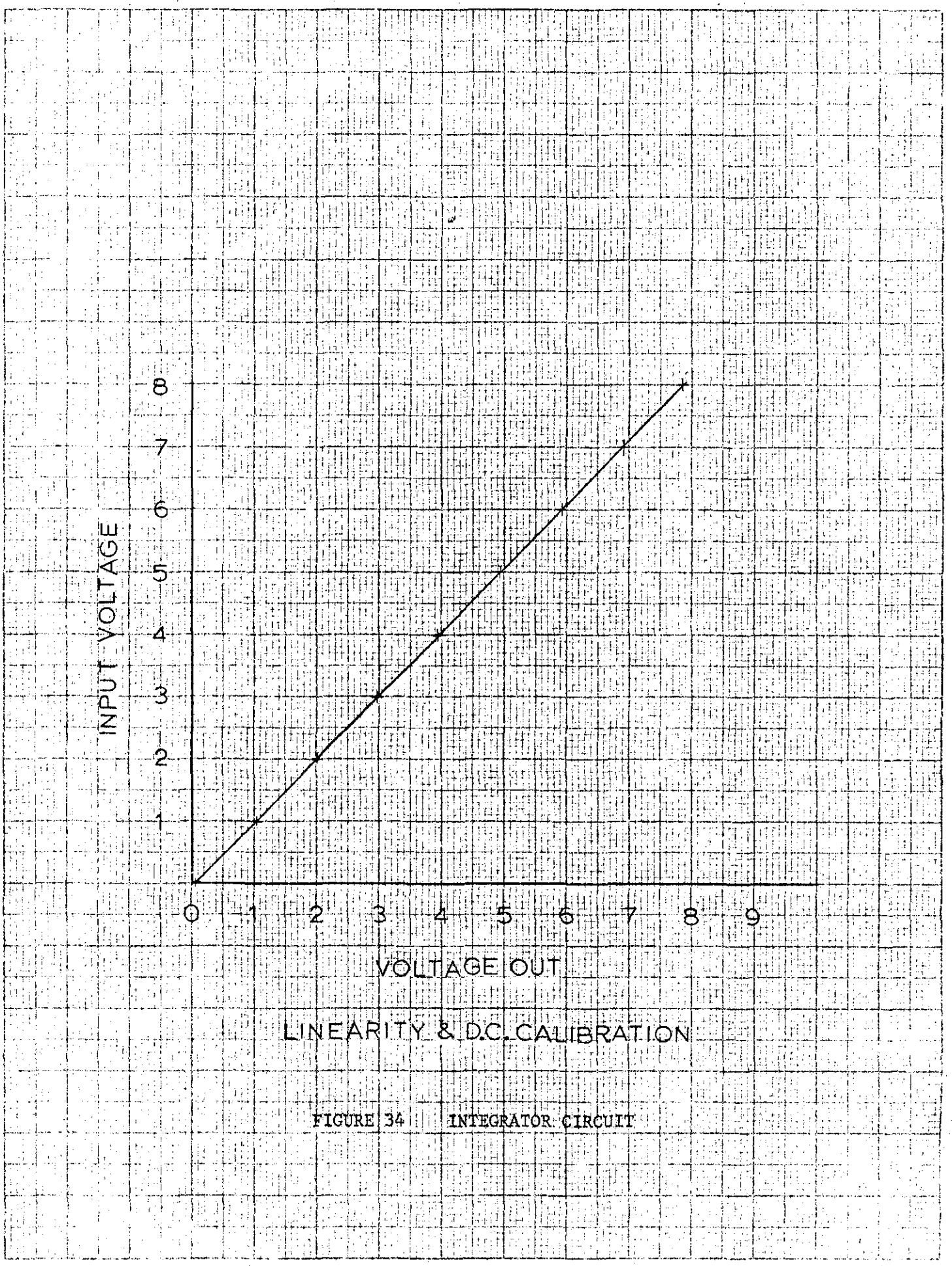

FIGURE 34 INTEGRATOR CIRCUIT